



華中師範大學
CENTRAL CHINA NORMAL UNIVERSITY



Central China
Center for Nuclear Theory
华中核理论中心



Institute of Particle Physics
粒子物理研究所



Machine Learning for Nuclear Theory

Long-Gang Pang 庞龙刚

Central China Normal University

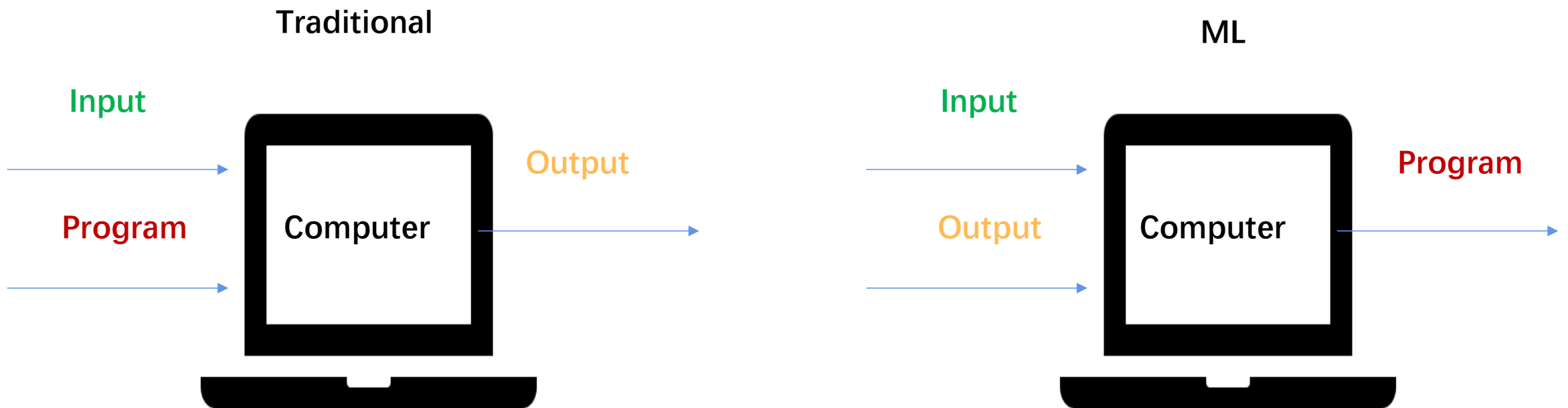
2025/5/18 WuHan

Inaugural Symposium of the CentralChina Center for Nuclear Theory(C3NT)
on Frontiers in Nuclear Theory

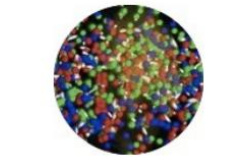
What is Machine Learning

The field of study that gives computers the ability to learn without being explicitly programmed.

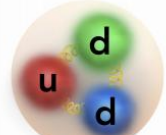
—Samuel 1959



ML for nuclear physics



Hot and Dense
Nuclear Matter



Hadrons



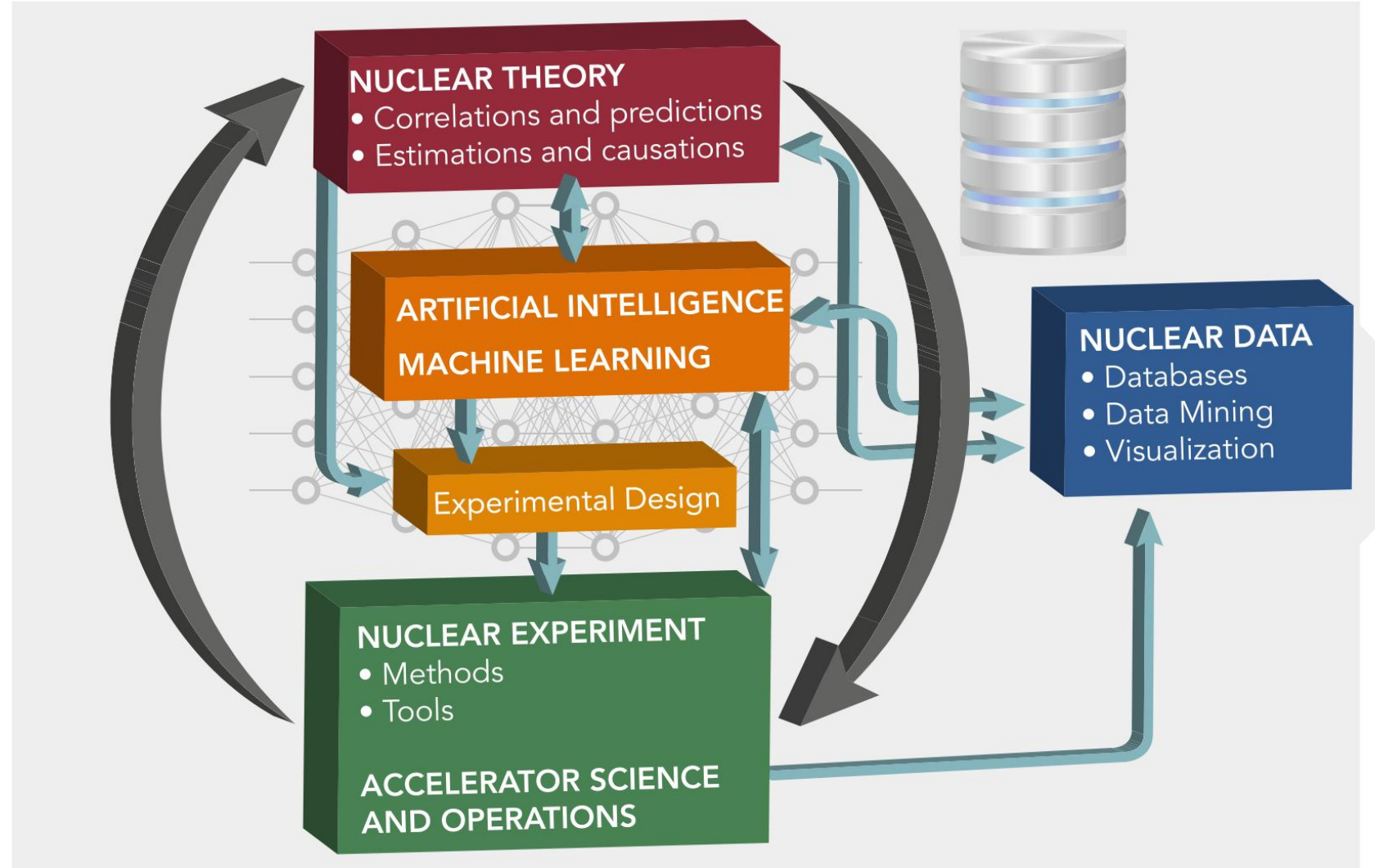
Atomic Nucleus



Nuclei in the Cosmos

u	c	t	γ	H
d	s	b	g	
v _e	v _{μ}	v _{τ}	Z ⁰	
e	μ	τ	W ⁺	W ⁻

Fundamental Interactions



RMP 94, 031003 (2022) Amber Boehnlein, et al.

ML for Nuclear mass and other properties

ANN: Gazula1992NPA, Athanassopoulos2004NPA, Bayram2014ANE, Zhang2017JPG,
Ming2022NST, Yüksel2021IJMPE, Li2022PRC

BNN: Utama2016PRC, Niu2018PLB, Niu2019PRC, Niu2022PRCL, Rodriguez2019EPL,
Rodriguez2019JPG

BGP: Neufcourt2018,2020PRC, Neufcourt2019PRL, Yüksel2024PRC

CNN: Yang2023PRC

LightGBM: Gao2021NST

KRR: Wu2020PRC, Wu2021PLB

NBP: Liu2021PRC, Xie2024PRC

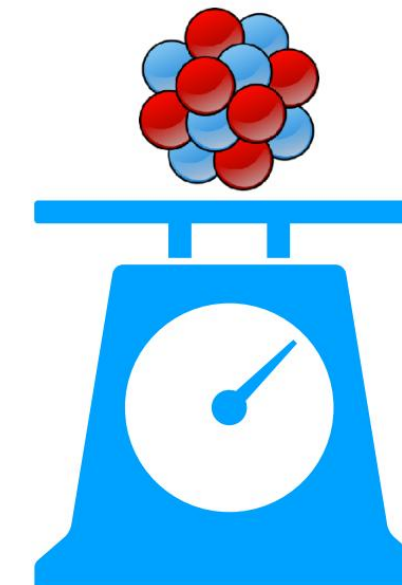
RBF: Wang2011PRC, Niu2013,2016PRC,2018SciB

SVM: Clark2006IJMPB

CLEAN: Morales2010PRC

...

from Prof. PengWei Zhao's slides



RNN, GRU and LSTM Models:
Amir Jalili, Feng Pan, Ai Xi Chen, and
Jerry P. Draayer, 2025

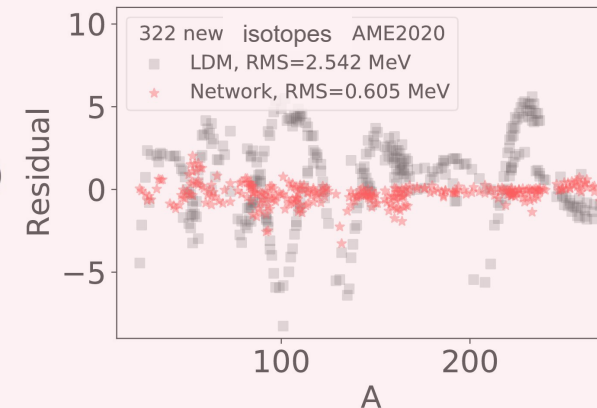
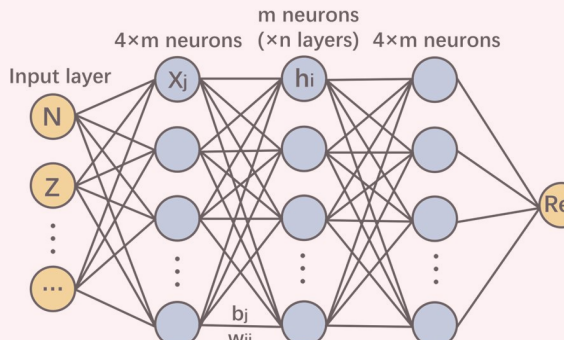
ML for Nuclear Charge Radius (Review)

Dong Xiaoxu; Geng Lisheng

- Naive Bayesian
- kernel ridge regression
- ANN

Z, N → mass, charge radius, ...

ML for Nuclear mass

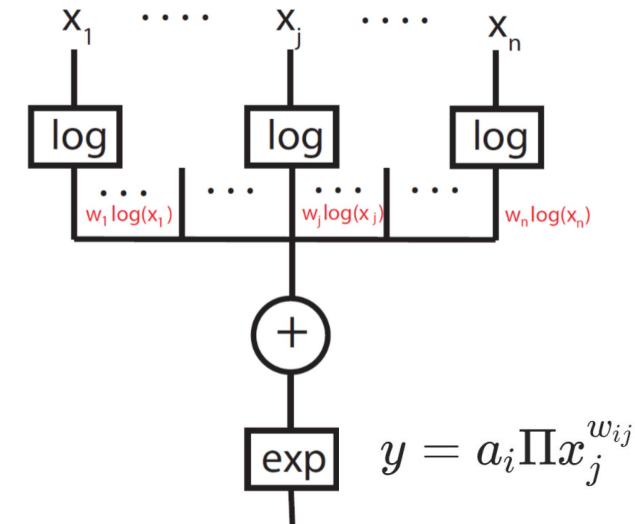


The Deep Neural Network

- 1 millions trainable parameters
- thought to be easy to overfit to training data
- in practice, it generalizes better than LDM

Li, Tong, Du, Pang, PRC 105 (2022) 6, 064306

Product-unit network



Babette D, Uwe J, Paulo S.A. F,
 John W. C. PLB 852(2024)138608

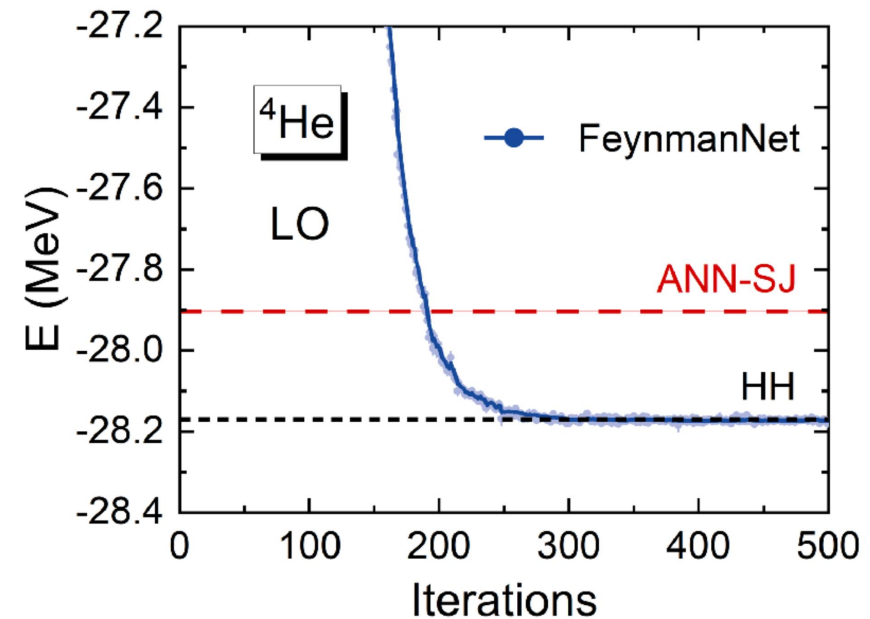
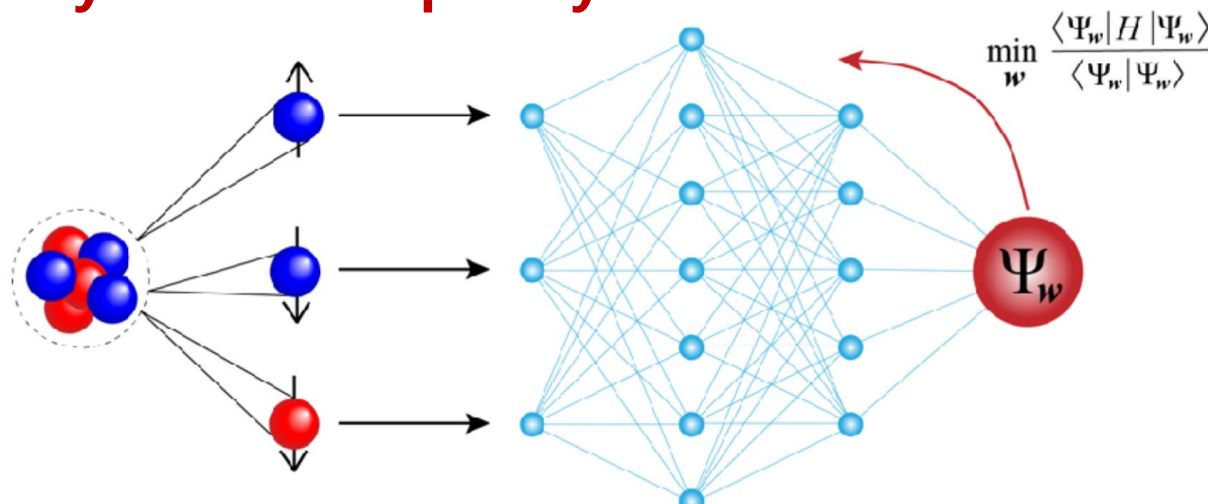
- complex valued x and w
- much fewer parameters
- better explanation

Ab initio calculations

$$\hat{H} = \sum_{i=1}^A \frac{-\nabla_i^2}{2m_N} + \sum_{i < j} v_{ij} + \sum_{i < j < k} V_{ijk}, \quad \longrightarrow$$

E_0 : ground state mass
 Ψ_0 : ground state wave function

Polynomial complexity



ANN-SJ: Adams, et al., PRL 127, 022502 (2021)

VMC-ANN: Alex Gnech, et al. Few Body Syst. 63 (2022) 1, 7

FeynmanNet: Yang, PWZ*, PRC 107, 034320 (2023)

Nuclear EDFT from machine learning

Nuclear energy density functionals from machine learning

X. H. Wu (吴鑫辉) , Z. X. Ren (任政学) , and P. W. Zhao (赵鹏巍) *

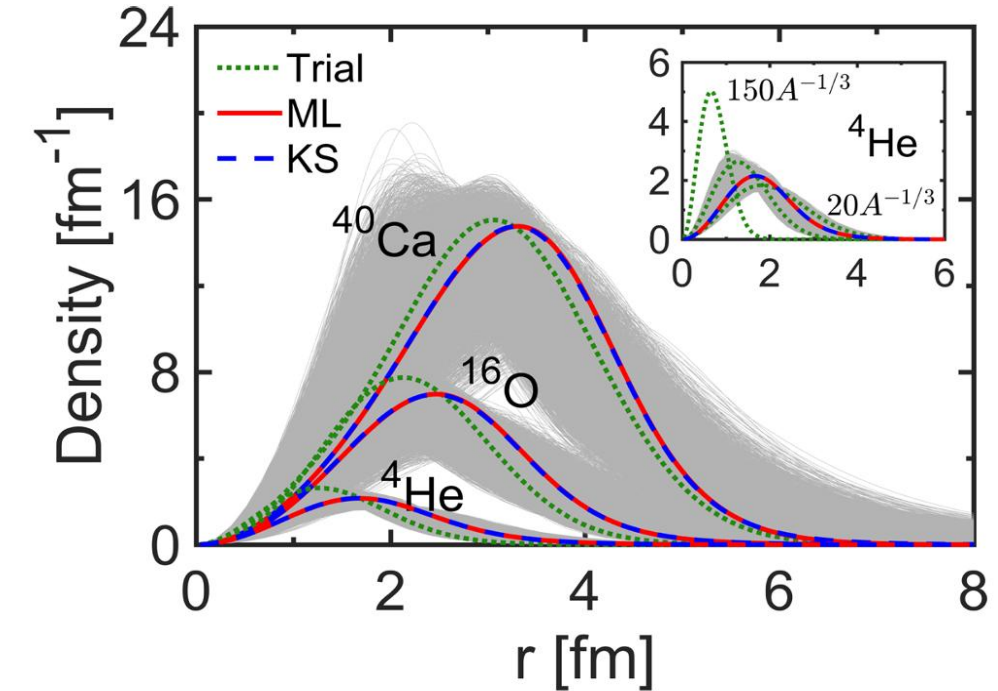
Kernel ridge regression: $\rho(r) \rightarrow E_{kin}$

$$E_{kin}^{ML}[\rho(\mathbf{r})] = \sum_{i=1}^m \omega_i K(\rho_i, \rho).$$

$$K(\rho, \rho') = \exp[-||\rho(\mathbf{r}) - \rho'(\mathbf{r})||^2 / (2AA'\sigma^2)].$$

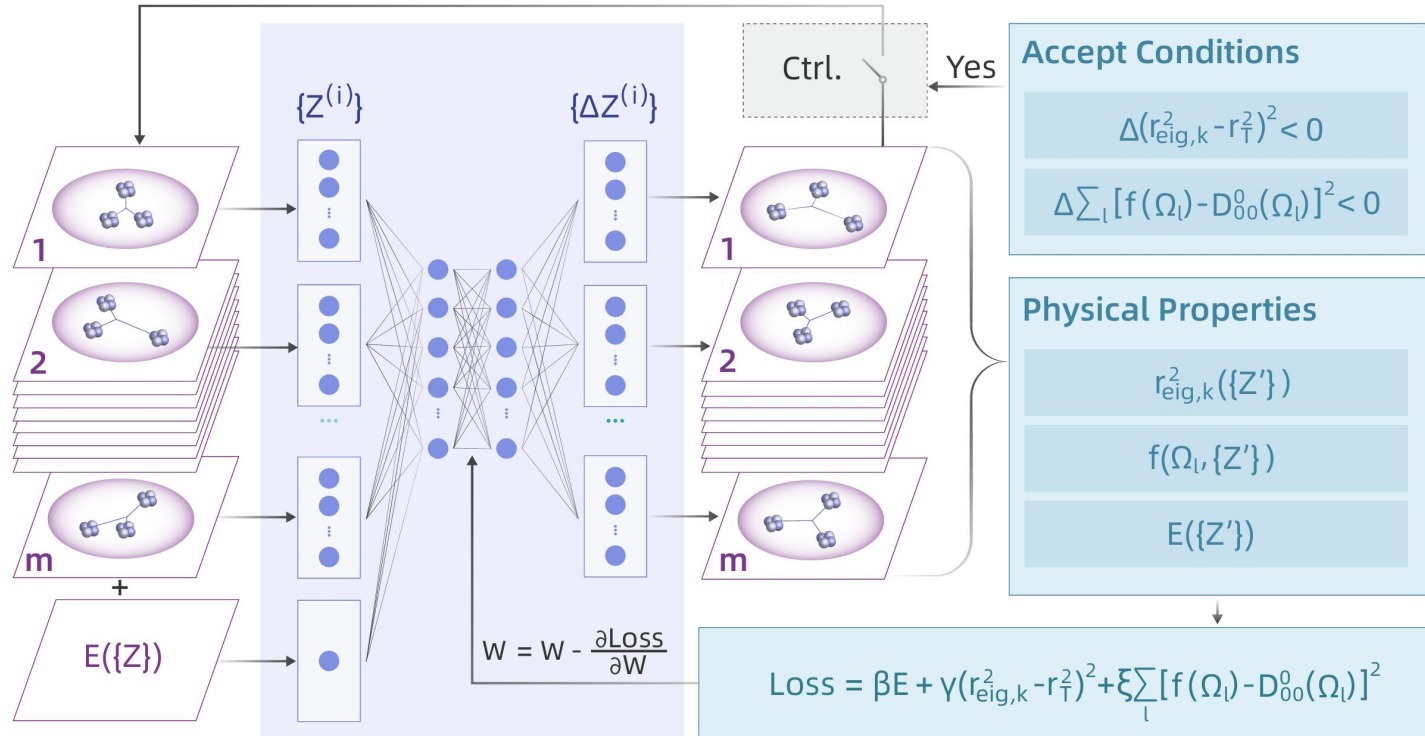
Loss function:

$$L(\boldsymbol{\omega}) = \sum_{i=1}^m (E_{kin}^{ML}[\rho_i] - E_{kin}[\rho_i])^2 + \lambda ||\boldsymbol{\omega}||^2,$$



By learning the kinetic energy as a functional of the nucleon density alone, a robust and accurate orbital-free density functional for nuclei is established.

Control NN for 3- α breathing in C12



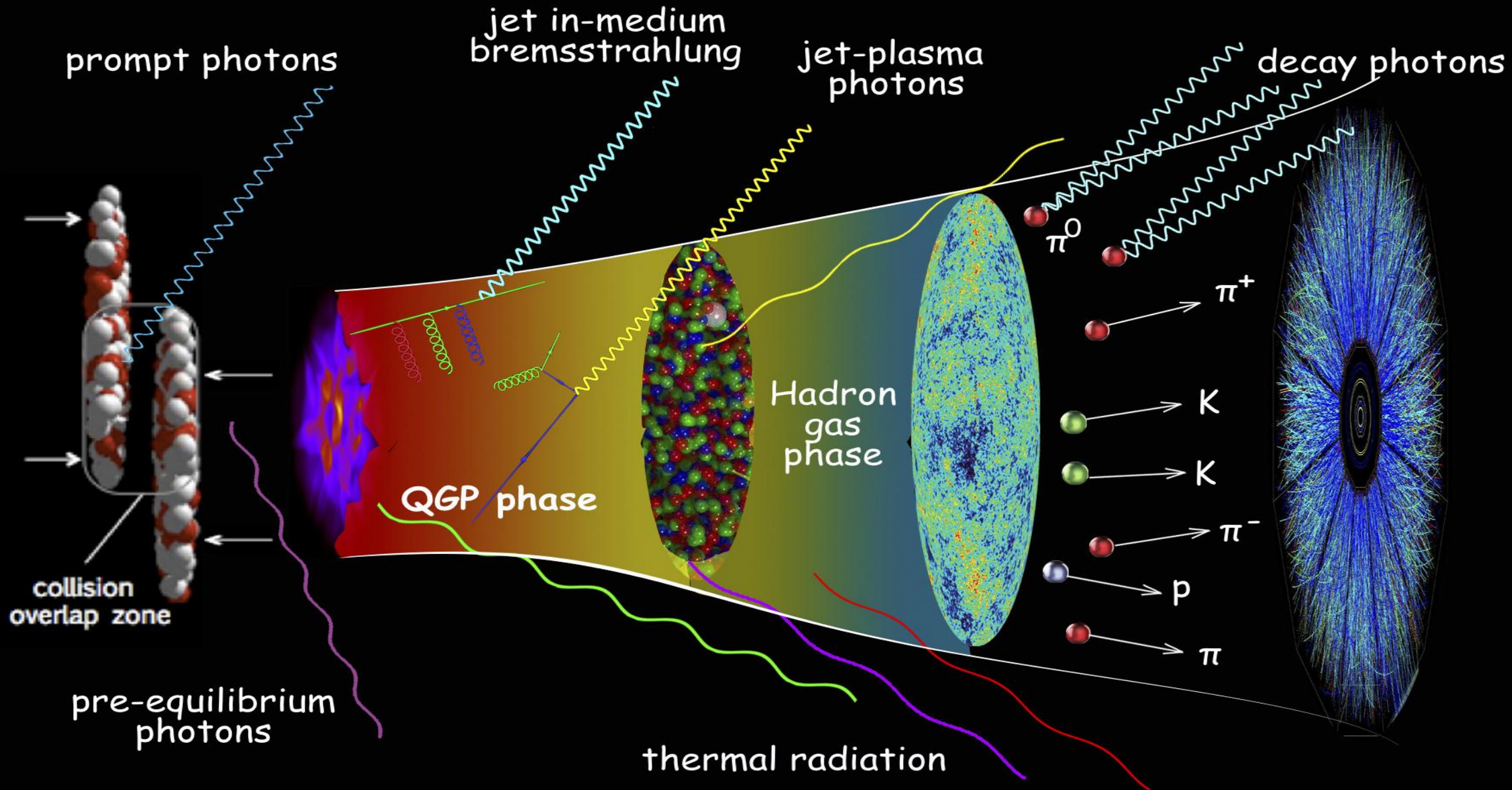
Evidence for Three- α Breathing Modes Uncovered by Control Neural Network

Zheng Cheng^{1,2}, Mengjiao Lyu^{1,2,*}, Takayuki Myo^{3,4}, Hisashi Horiuchi⁴, Hiroshi Toki⁴, Zhongzhou Ren^{5,6}, Masahiro Isaka⁷, Mengyun Mao^{1,2}, Hiroki Takemoto⁸, Niu Wan⁹, Wenlong You^{1,2}, and Qing Zhao¹⁰

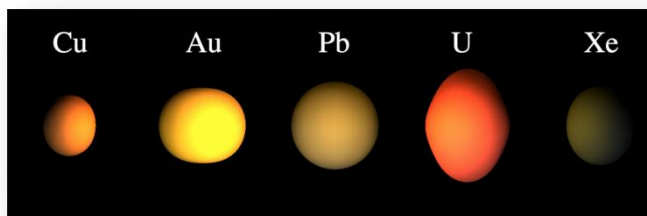
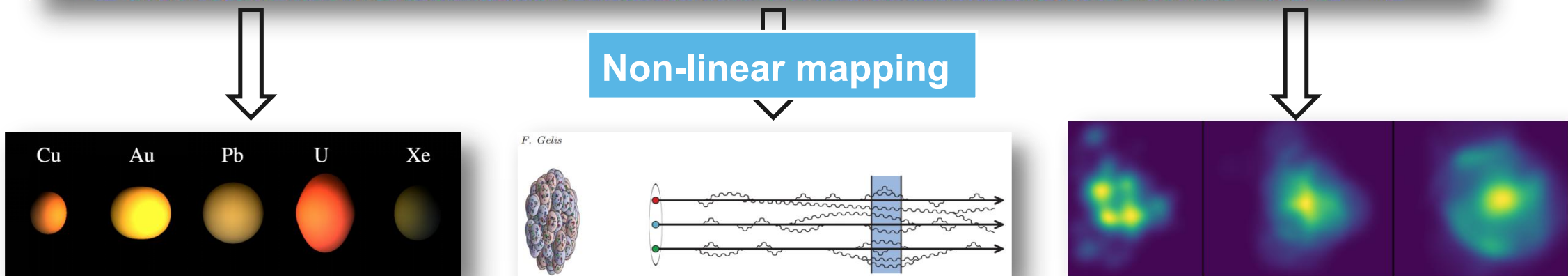
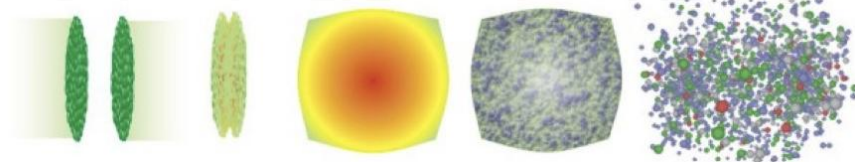
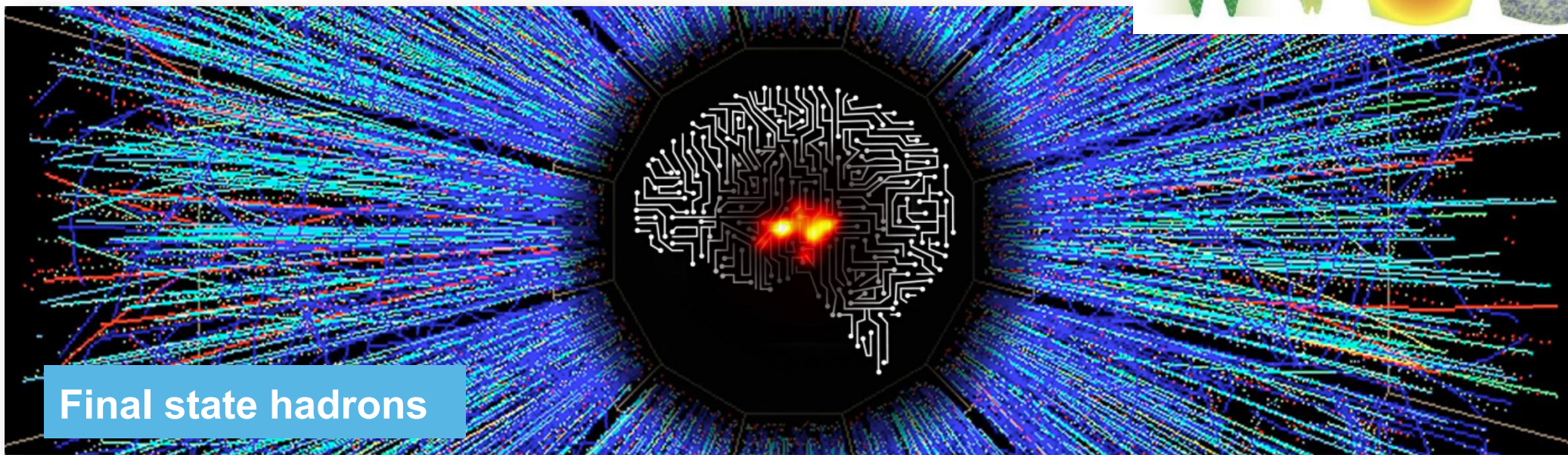
In each iteration, **a new basis set $\{Z'\}$ is obtained and diagonalized to yield the new total intrinsic wave function $\Psi(\{Z'\})$ and physical properties corresponding to each of the three constraints,**

$$\text{Loss} = \beta E + \gamma (r_{\text{eig},k}^2 - r_T^2)^2 + \xi \sum_{l=1}^L [f(\Omega_l) - D_{MK}^J(\Omega_l)]^2,$$

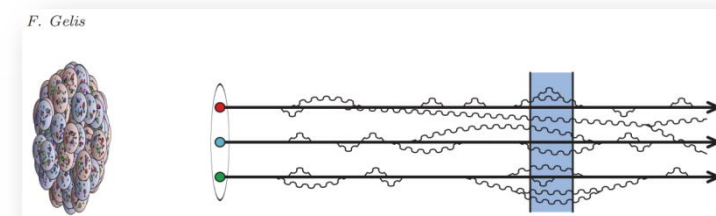
Constraints: (1) minimum eigen value (2) mean square radius (3) rotational symmetry



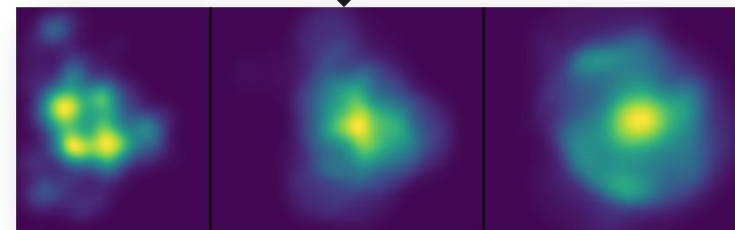
Inverse problems in HIC



(1) Nuclear Structure

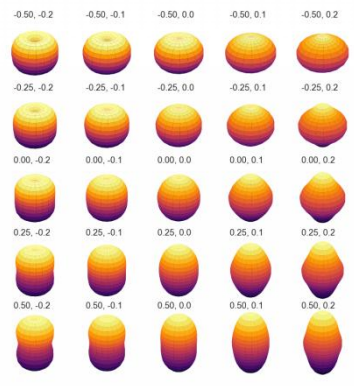


(2) Initial Parton Distribution



(3) QGP properties and EoS

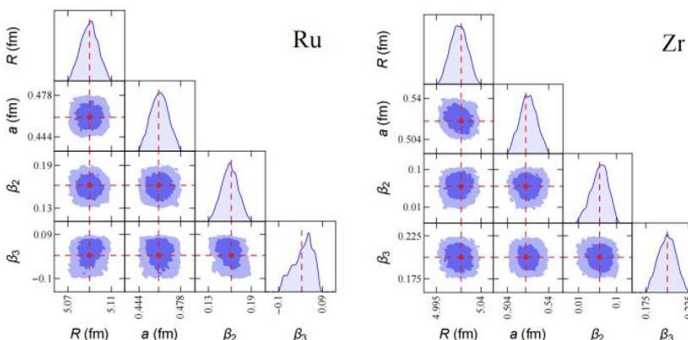
Nuclear Structure using HICs and ML



1. change β_2, β_4
2. A+A collision sim.
3. ML: final \rightarrow initial nuclear deformation

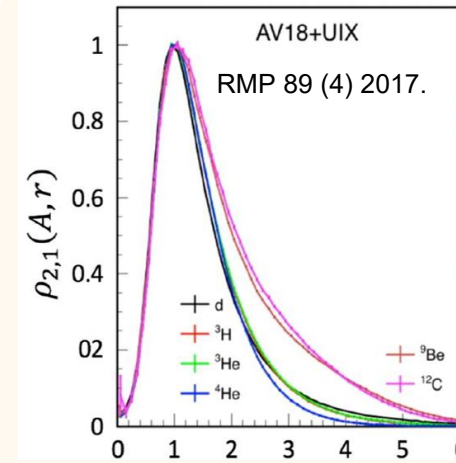
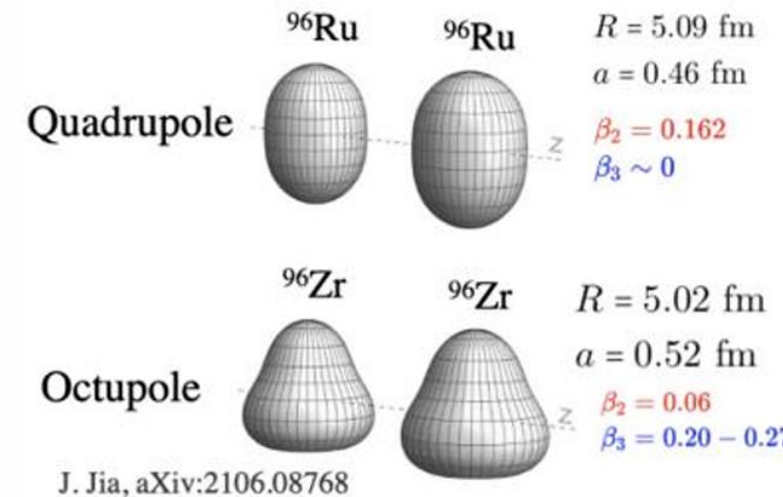
LG. Pang, K. Zhou and X.-N. Wang, arXiv:1906.06429

$$\mathbf{y}_{\text{Ru}} \equiv \{P_a^{\text{Ru}}, \varepsilon_{2,a}^{\text{Ru}}, \varepsilon_{3,a}^{\text{Ru}}, d_{\perp,a}^{\text{Ru}}\}_{a=1,\dots,40}$$



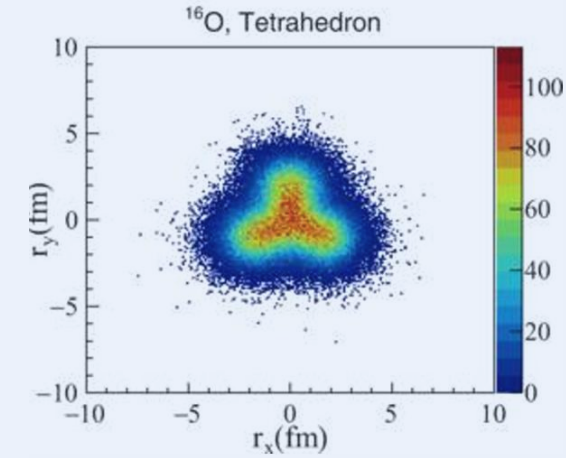
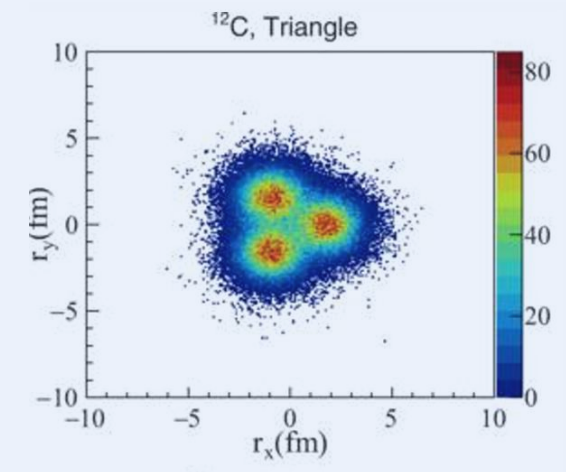
Single system works good

Y.Cheng, S.Shi, Y. Ma, H. S., K. Zhou, PRC107 (2023) 064909



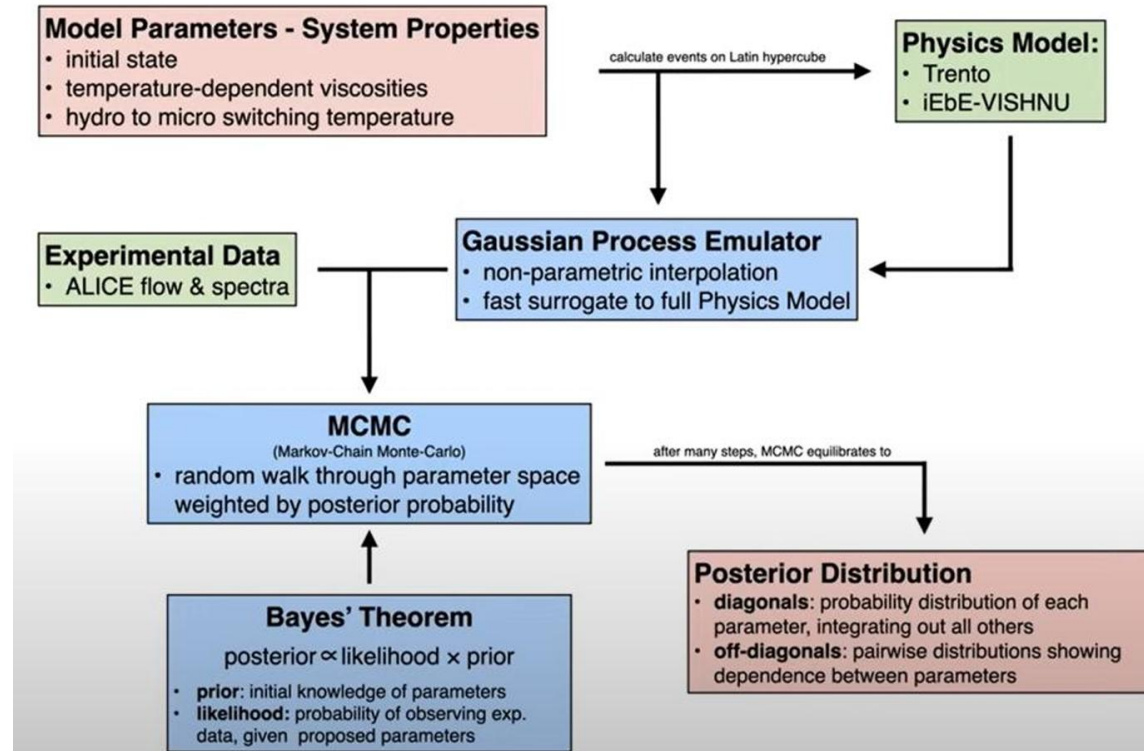
Y.J. Huang, Z. Meng, L.G. Pang, X.N. Wang, arXiv:2504.00790

α cluster in C and O



J He, W. He, Y.G. Ma, S. Zhang, PRC104, 044902

Bayesian analysis of HICs



Trento + IEBE-VishNew + UrQMD

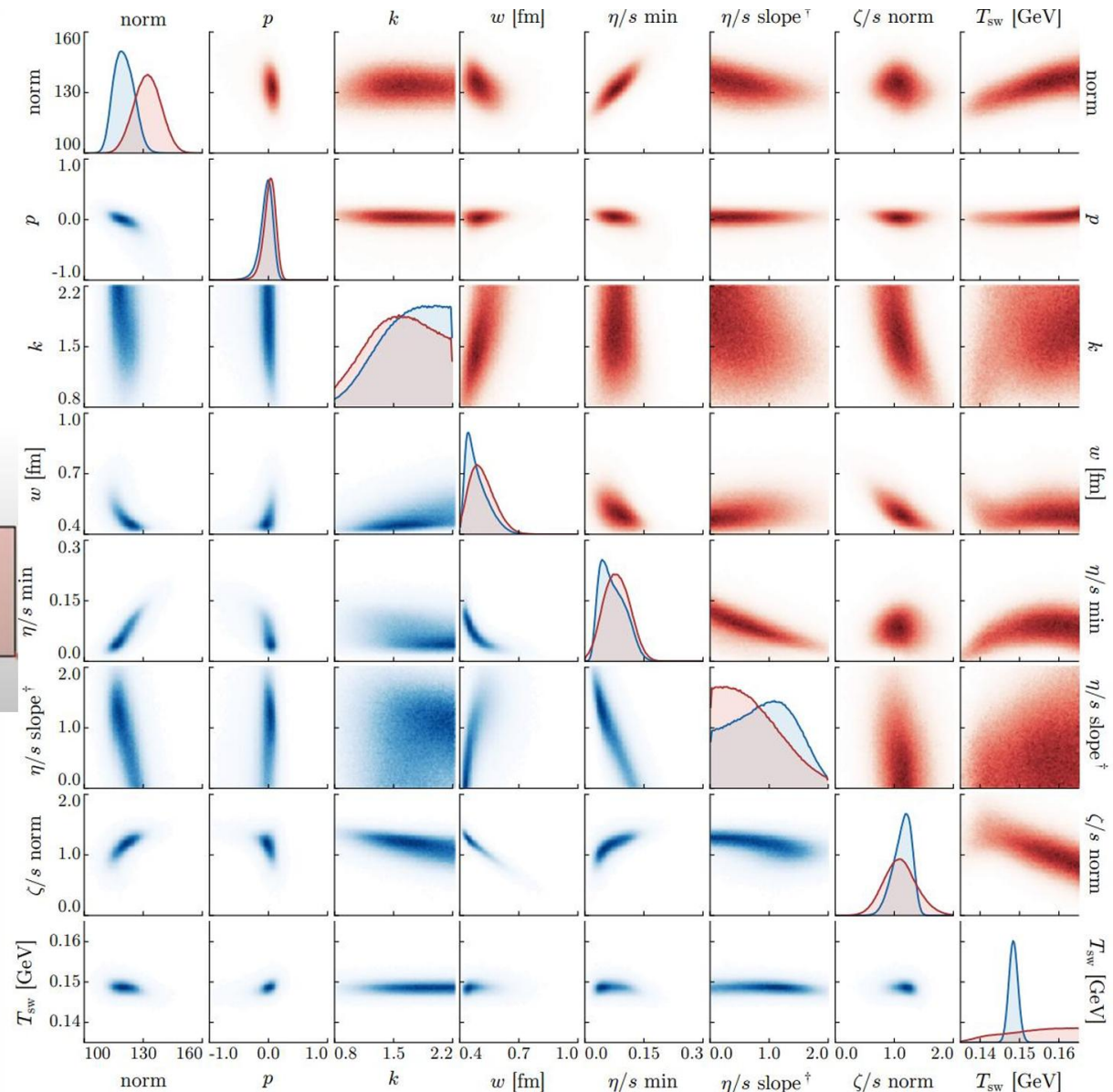
J. Bernhard, J. Morel, S. Bass, **Nat. Phys.** 15, 1113 (2019)

G. Nijs, W. Schee, U. Guersoy, R. Snellings, **PRC**103,054909;
JETSCAPE, **PRL**126,242301; U. Heinz+, 2302.14184 (VAH)
M. R. Heffernan, C. Gale, S. Jeon, J. Pauet, **PRC**109,065207;

.....
Jet quenching/diffusion:

Y. He, L. Pang, X. Wang, **PRL** 122 (25) 252302

M. Xie, W. Ke, H. Zhang, X. Wang, **PRC**108 (2023) L011901;



Bayesian analysis QCD EoS

$$c_s^2(\epsilon) = c_s^2(\epsilon_h) + \left(\frac{1}{3} - c_s^2(\epsilon_h) \right) \frac{X_0 x + x^2}{X_0 x + x^2 + X'^2} \quad (2.12)$$

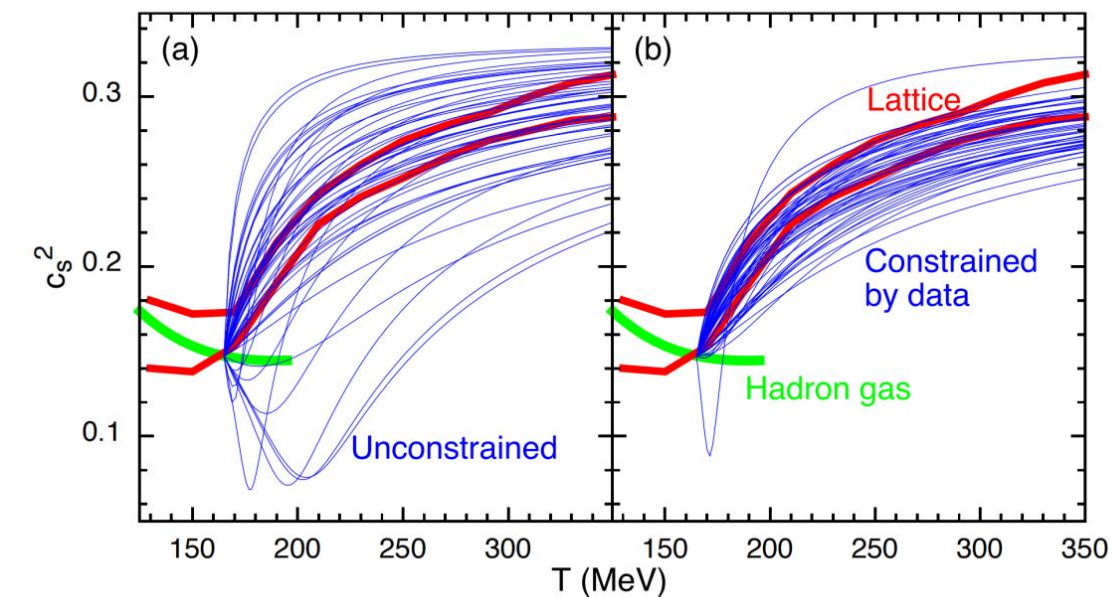
where $X_0 = \sqrt{12}RX'c_s(\epsilon_h)$, $x \equiv \ln \frac{\epsilon}{\epsilon_h}$, ϵ_h is the energy density at $T = 165$ MeV, R and X' are the two parameters in the EoS to be determined. Randomly choosing R and X' from the range $-0.9 < R < 2$ and $0.5 < X' < 5$ generate the

Likelihood:

$$P(D|\theta) = \prod_i \exp(-(z_i(\theta) - z_{i,\text{exp}})^2/2)$$

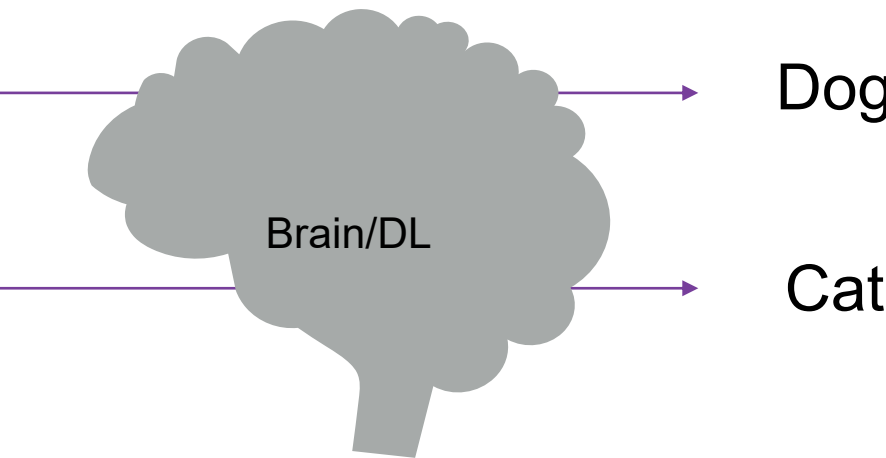
Posterior:

$$P(\theta | D) \propto P(D | \theta)P(\theta)$$



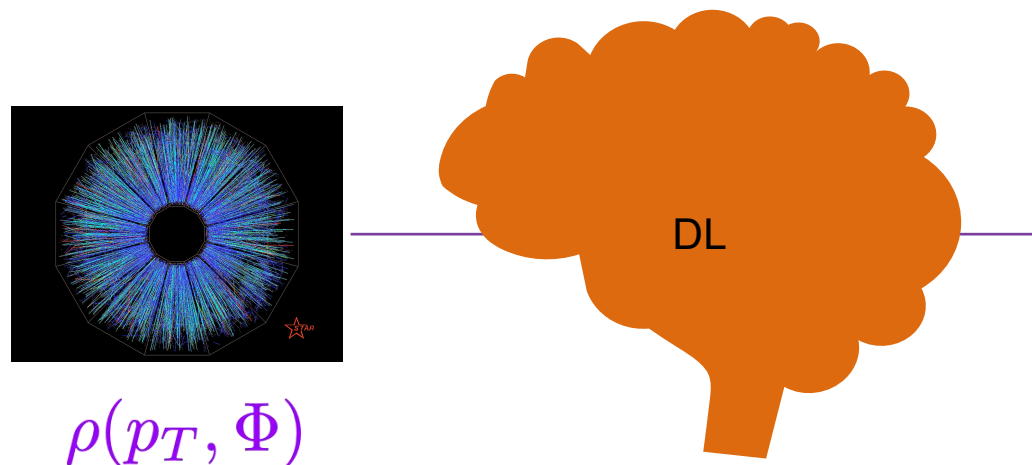
S. Pratt, E. Sangaline, P. Sorensen, H. Wang, PRL. 114 (2015) 202301.

DL for inverse/variational problems in HICs



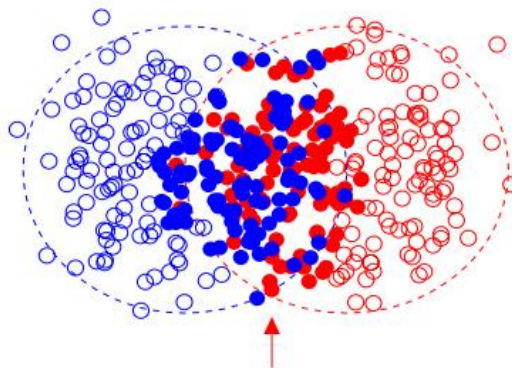
Human brains are not optimized for processing high-dimensional scientific data. Deep neural network can be trained:

- (i) to **identify optimal feature combinations**
- (ii) to **represent variational functions**



QCD phase structure/EoS,
Nuclear structure (deformation, nn
SRC, neutron skin, α clusters),
shear/bulk viscosity of QGP, CME ...

Theoretical model: relativistic hydro

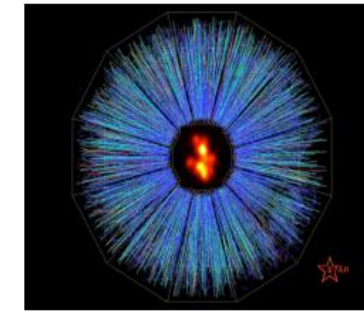


Initial condition

$$\nabla_\mu T^{\mu\nu} = 0 \quad \longrightarrow$$

$$T^{\mu\nu} = (\varepsilon + P)u^\mu u^\nu - Pg^{\mu\nu} + \pi^{\mu\nu}$$

EoS



Viscosity

Name of CLVisc:

1. CCNU-LBNL Viscous Hydro, CCNU = Central China Normal University
2. A 3+1D viscous hydro parallelized on GPU using OpenCL

Purpose: Describe the [non-equilibrium space-time evolution](#) of hot QCD matter

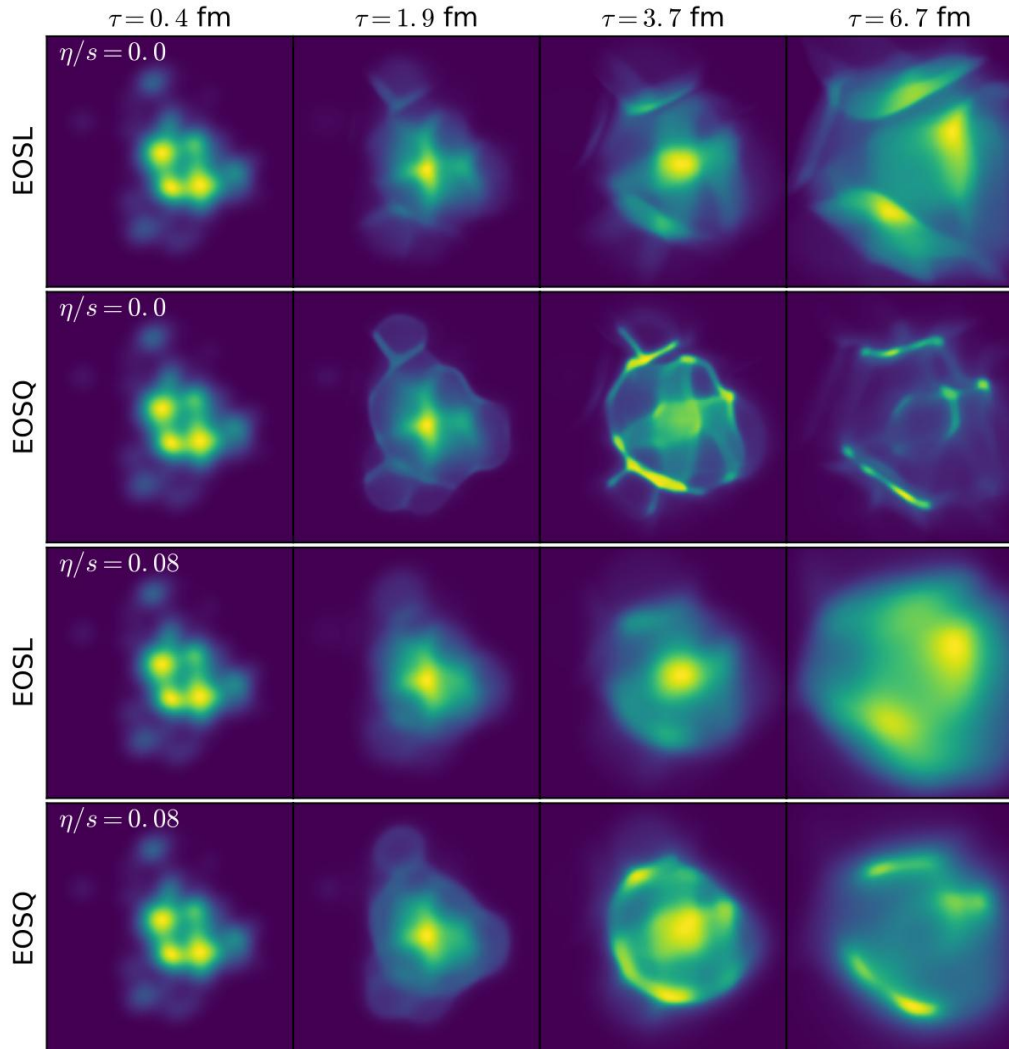
Feature: **100 times faster** than using a single core CPU.

L.G. Pang, Q. Wang and X. N. Wang, PRC 86 (2012) 024911

L.G. Pang, B.W. Xiao, Y. Hatta, X.N.Wang, PRD 2015

L.G. Pang, H.Petersen, XN Wang, PRC97(2018)no.6,064918

CLVisc for different EoS



$\eta/s = 0$ (shear viscosity over entropy density)
Lattice QCD EoS (smooth cross over)

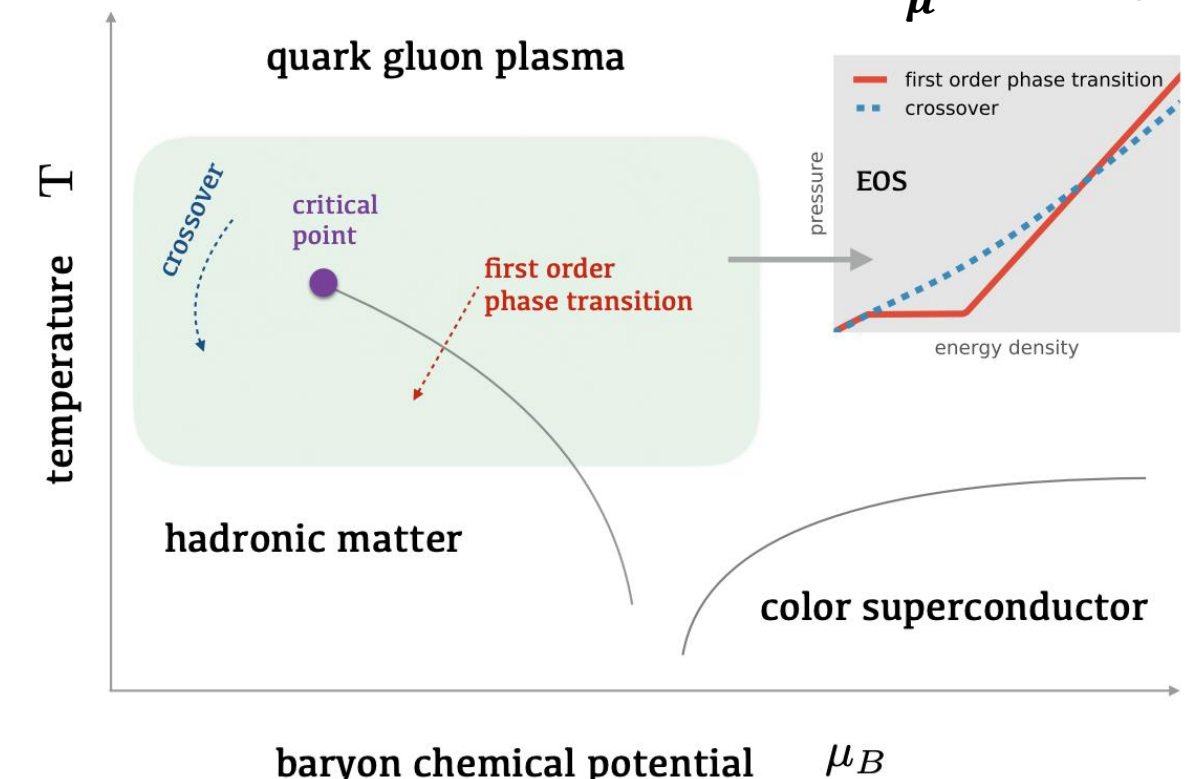
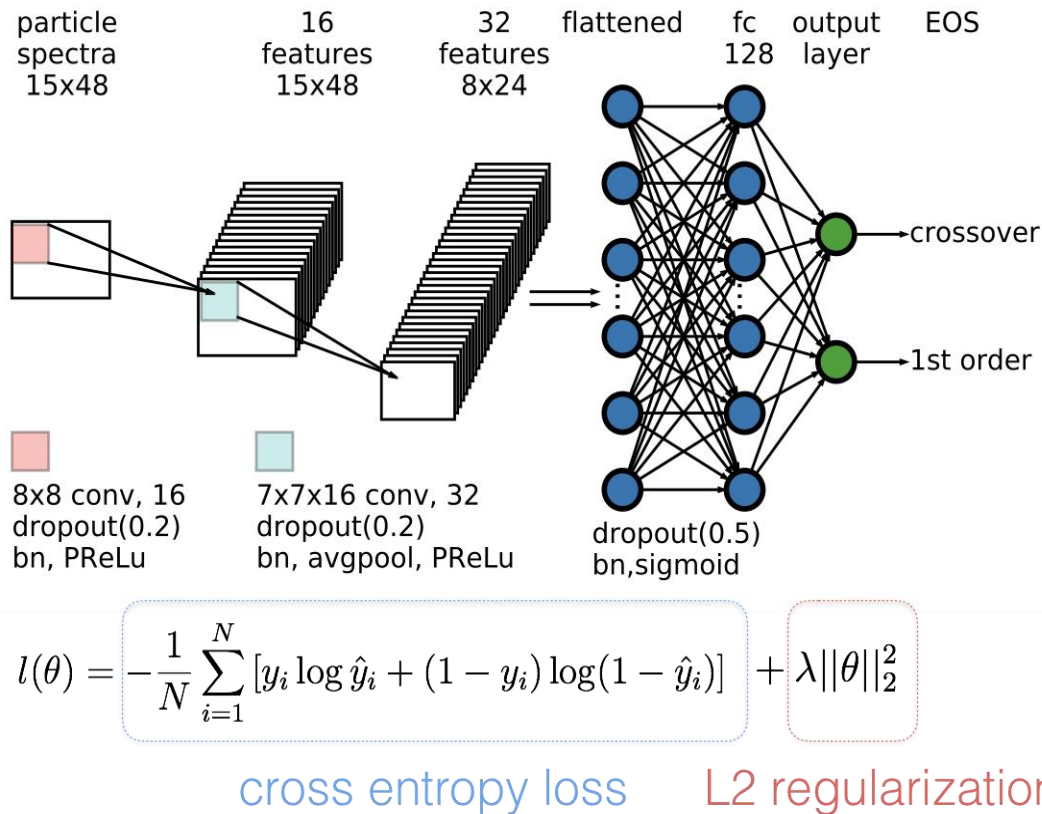
$\eta/s = 0$ (ideal hydro)
First order phase transition

$\eta/s = 0.08$ (viscous hydro)
Lattice QCD EoS (smooth cross over)

$\eta/s = 0.08$
First order phase transition

It is unknown whether the information of EoS survives the complex dynamical evolution of HICs and exists in each single event of the final state output.

EoS for different phase transition types

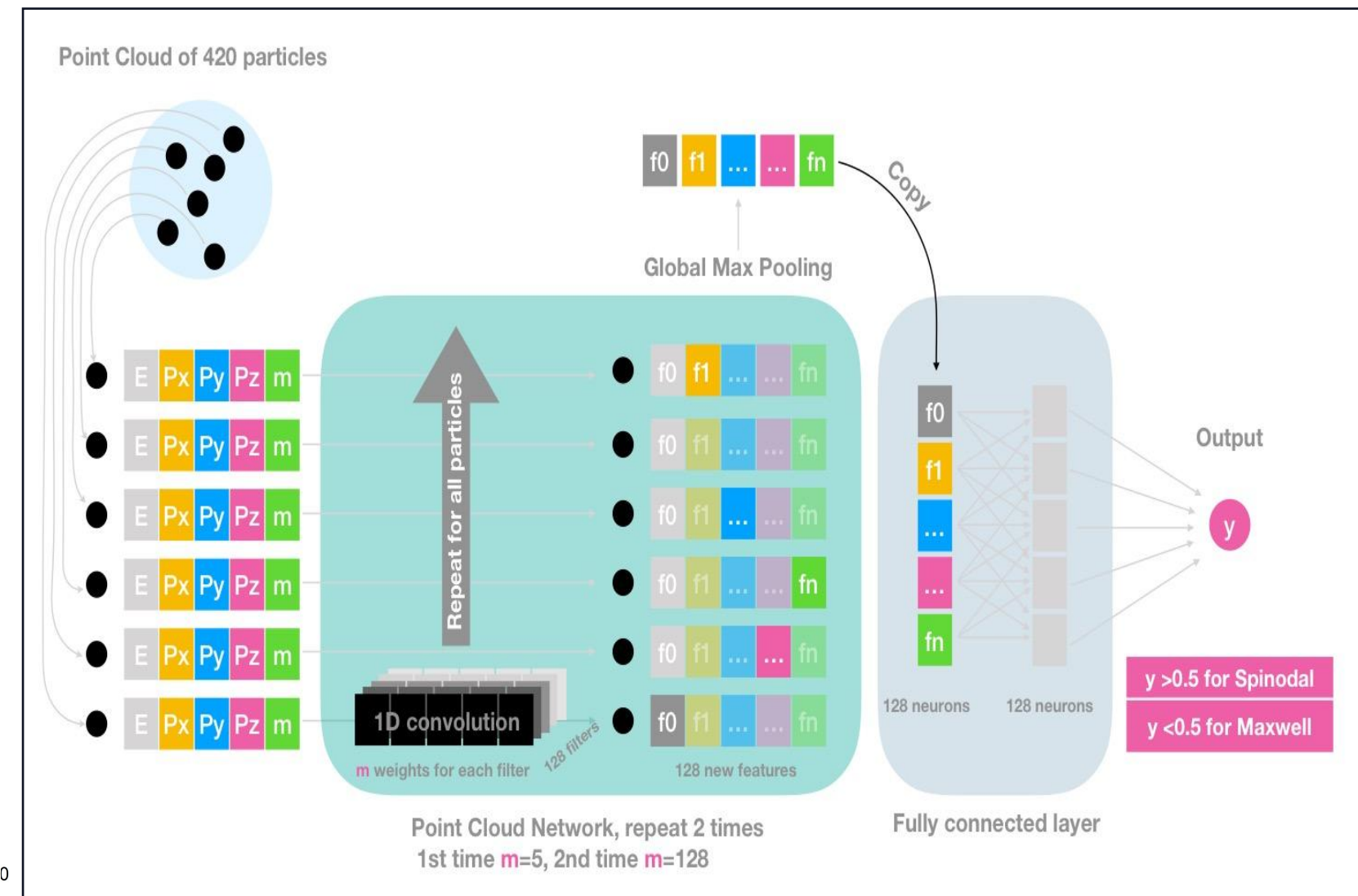
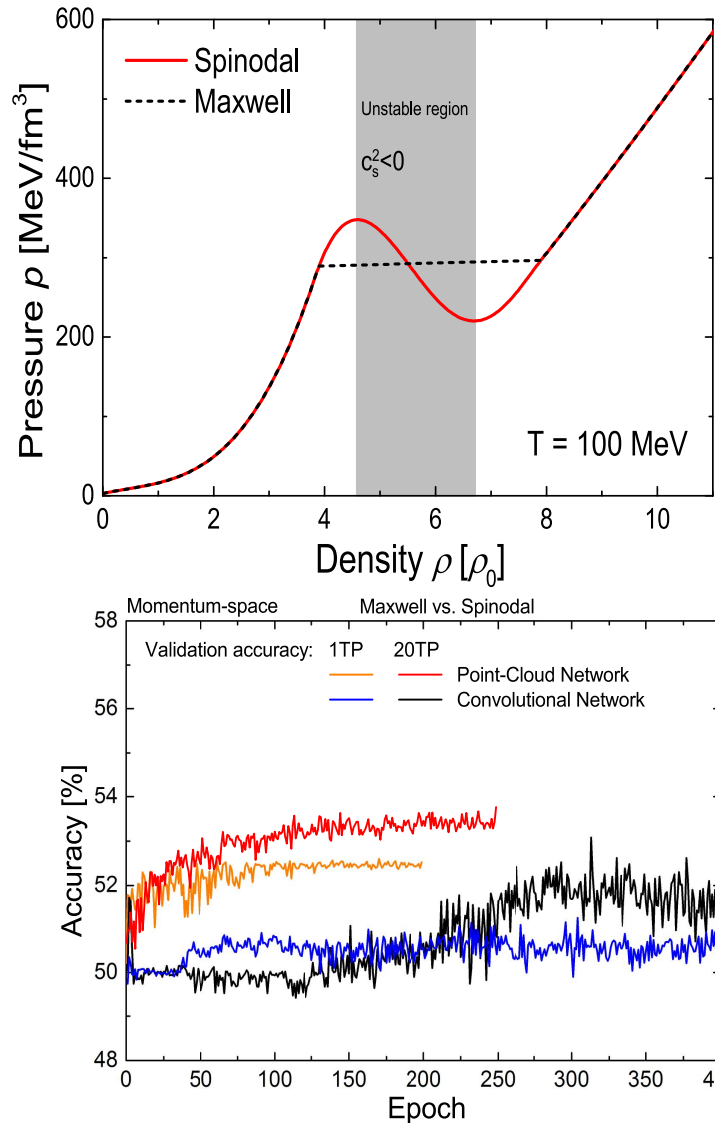


DL helps to decode the information of QCD phase transition in the QCD EoS (>93% accuracy).

Nature Communications 2018, **LG. Pang**, K.Zhou, N.Su, H.Petersen, H. Stoecker, XN. Wang.



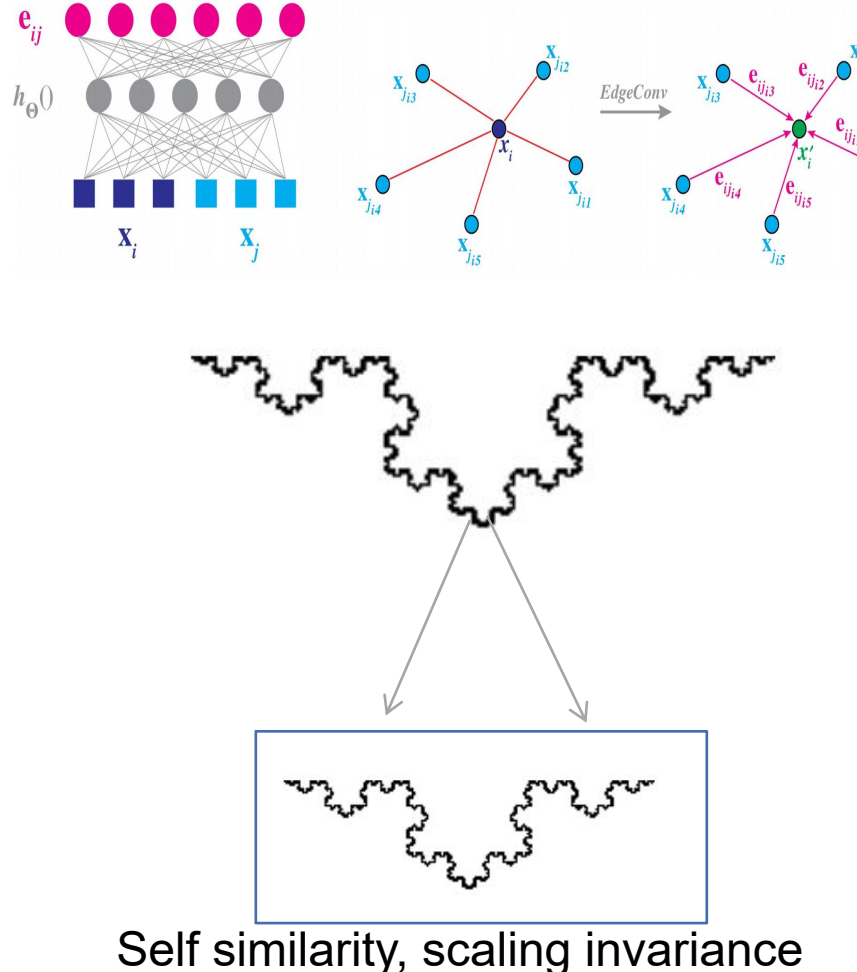
Spinodal vs Maxwell 1st order phase transition



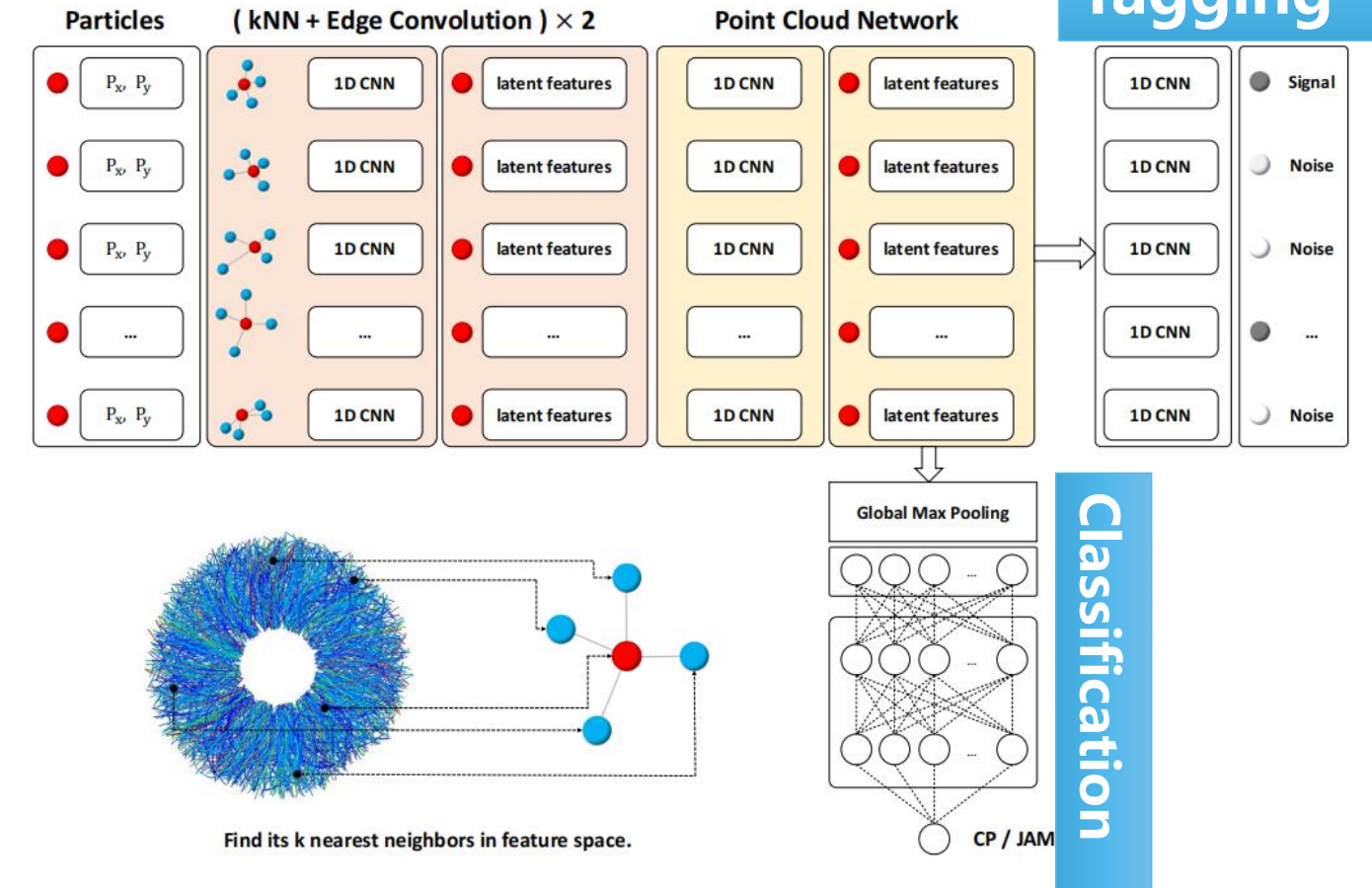
J. Steinheimer, L.G. Pang, K. Zhou, V. Koch and J. Randrup, JHEP 12 (2019) 122



Looking for self similarity in momentum space



Dynamical Edge Convolution Network



PLB 827(2022) 137001, Y.-G. Huang, L.-G. Pang, X.F. Luo and X.-N. Wang

Active learning to map out unphysical EoS

$$(\mu_{BC}, \alpha_{\text{diff}}, w, \rho) \mapsto P(T, \mu_B) \mapsto \{\text{acceptable, unstable, acausal}\}.$$

4 parameters from 3D Ising model

QCD EoS

Lables for classification

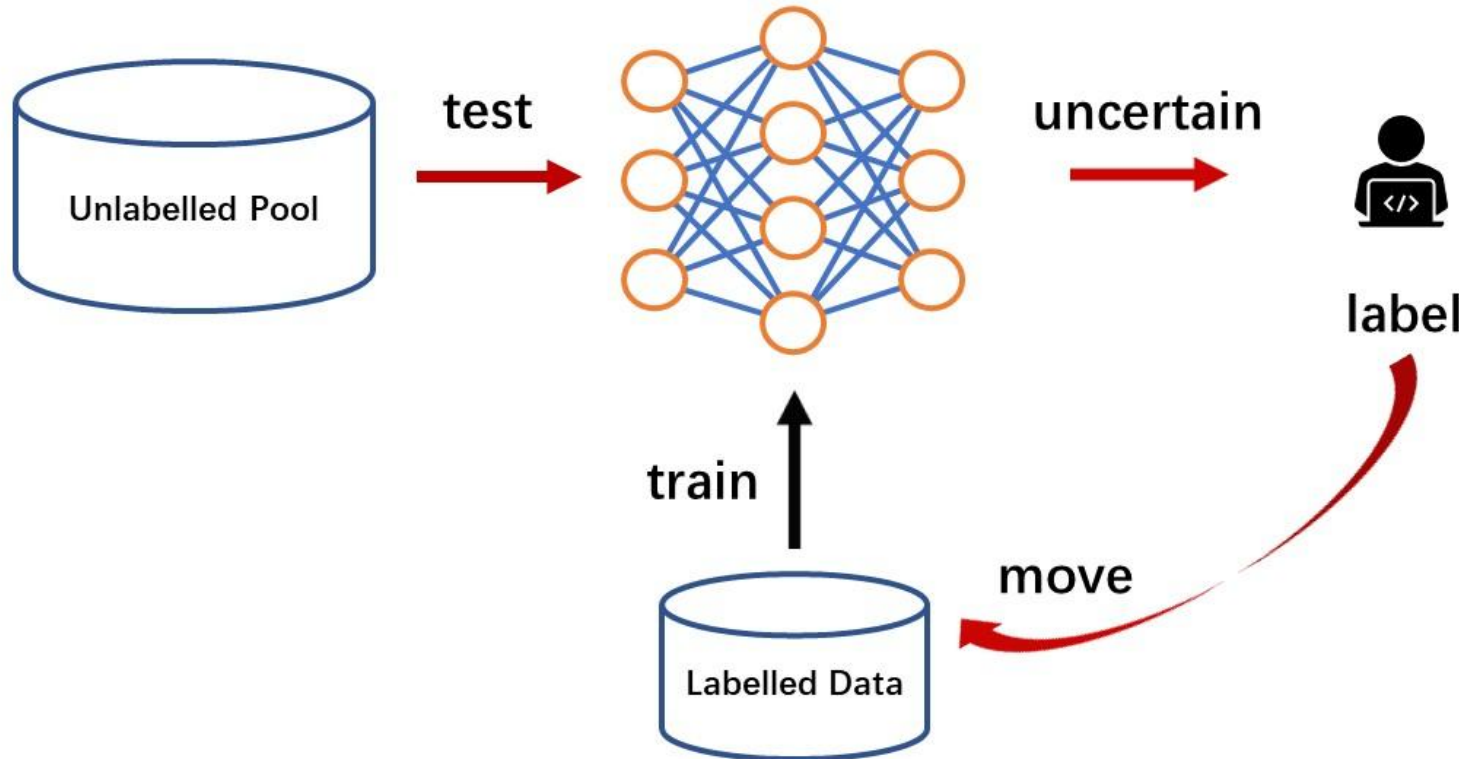
Acceptable = Stable + Causal

$$P, s, \varepsilon, n_B, \chi_2^B, \left(\frac{\partial S}{\partial T} \right)_{n_B} > 0, \quad 0 \leq c_s^2 \leq 1.$$

D. Mroczek, M. Hjorth-Jensen, J. Noronha-Hostler, P. Parotto, C. Ratti, and R. Vilalta, PRC 107, 054911

Active learning

Achieve high performance with much fewer data ($O(10^2)$)



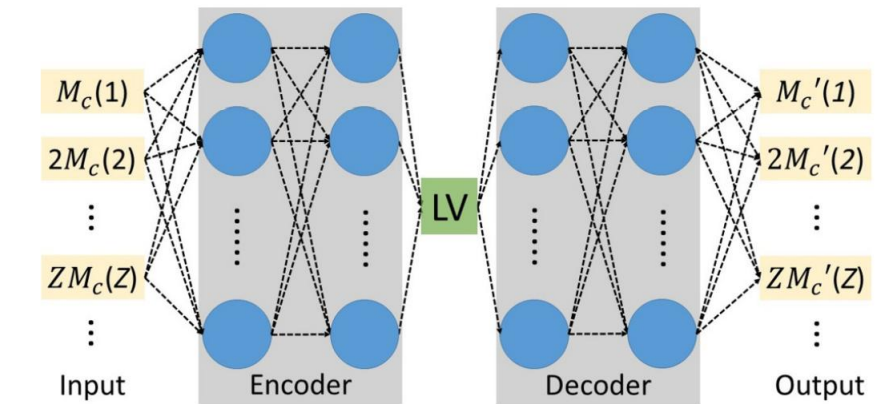
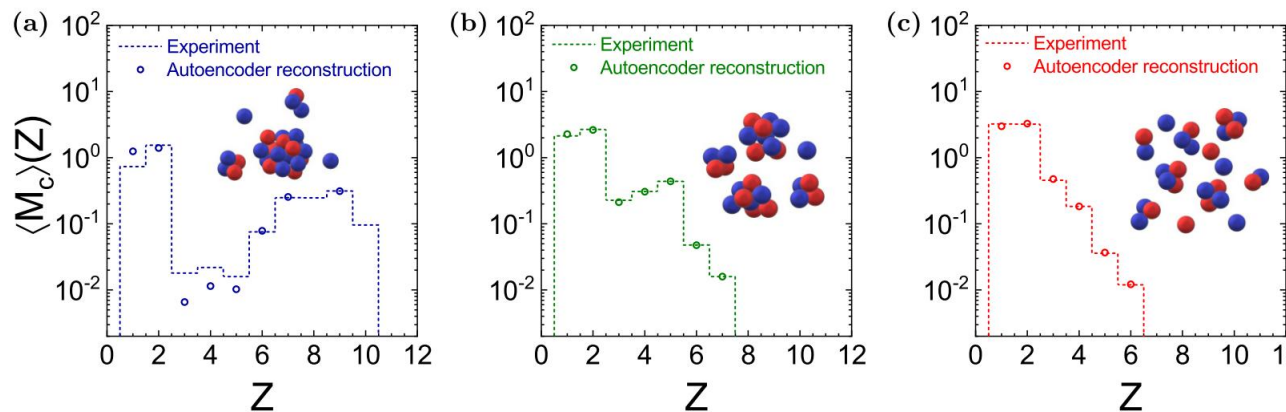
D. Mroczek, M. Hjorth-Jensen, J. Noronha-Hostler, P. Parotto, C. Ratti, and R. Vilalta, PRC 107, 054911

Auto Encoder for order parameter

PHYSICAL REVIEW RESEARCH 2, 043202 (2020)

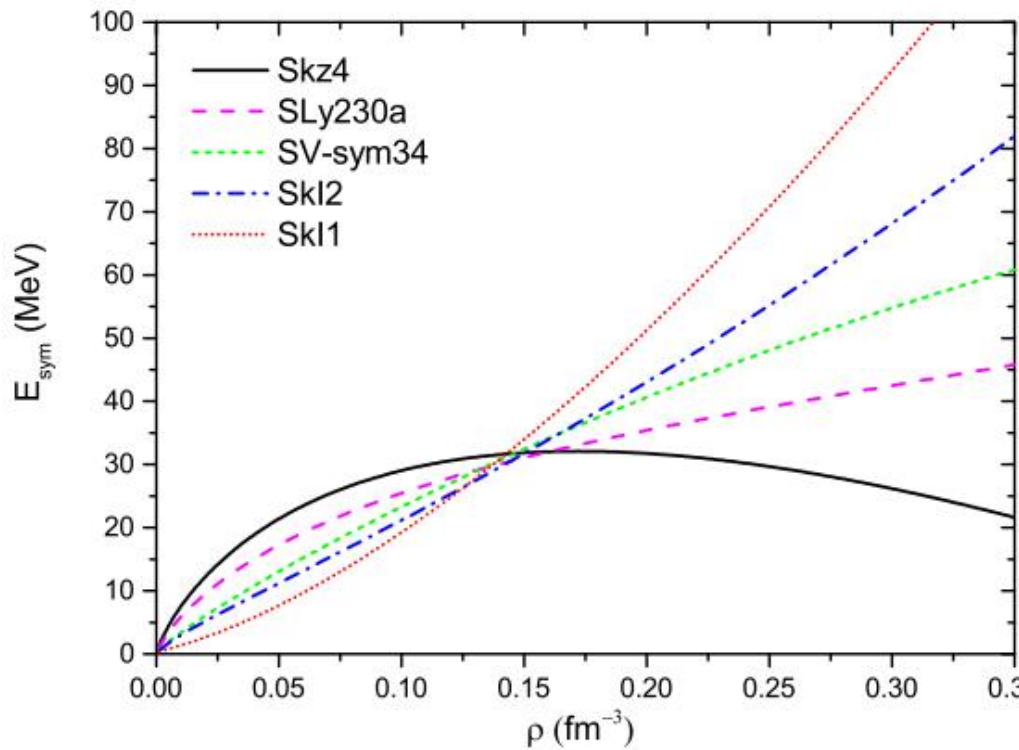
Nuclear liquid-gas phase transition with machine learning

Rui Wang^{1,2,*}, Yu-Gang Ma,^{1,2,†}, R. Wada,³, Lie-Wen Chen⁴, Wan-Bing He,¹, Huan-Ling Liu,², and Kai-Jia Sun^{3,5}

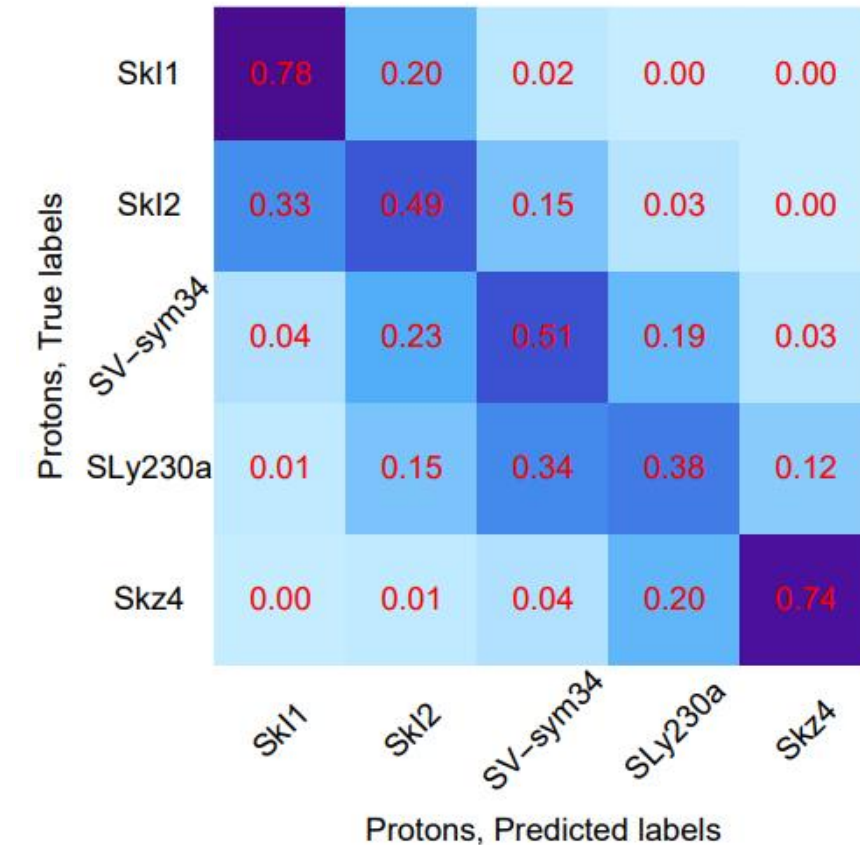


Nuclear EoS at high density region

Skyrme potential + IMQMD



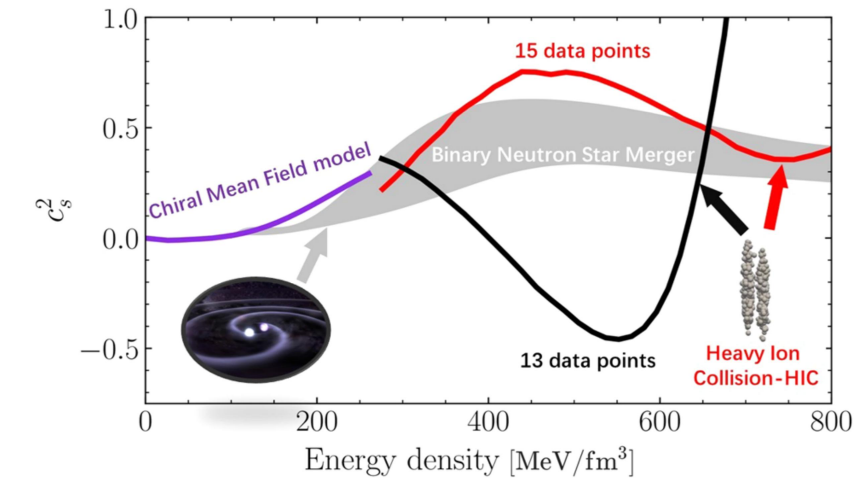
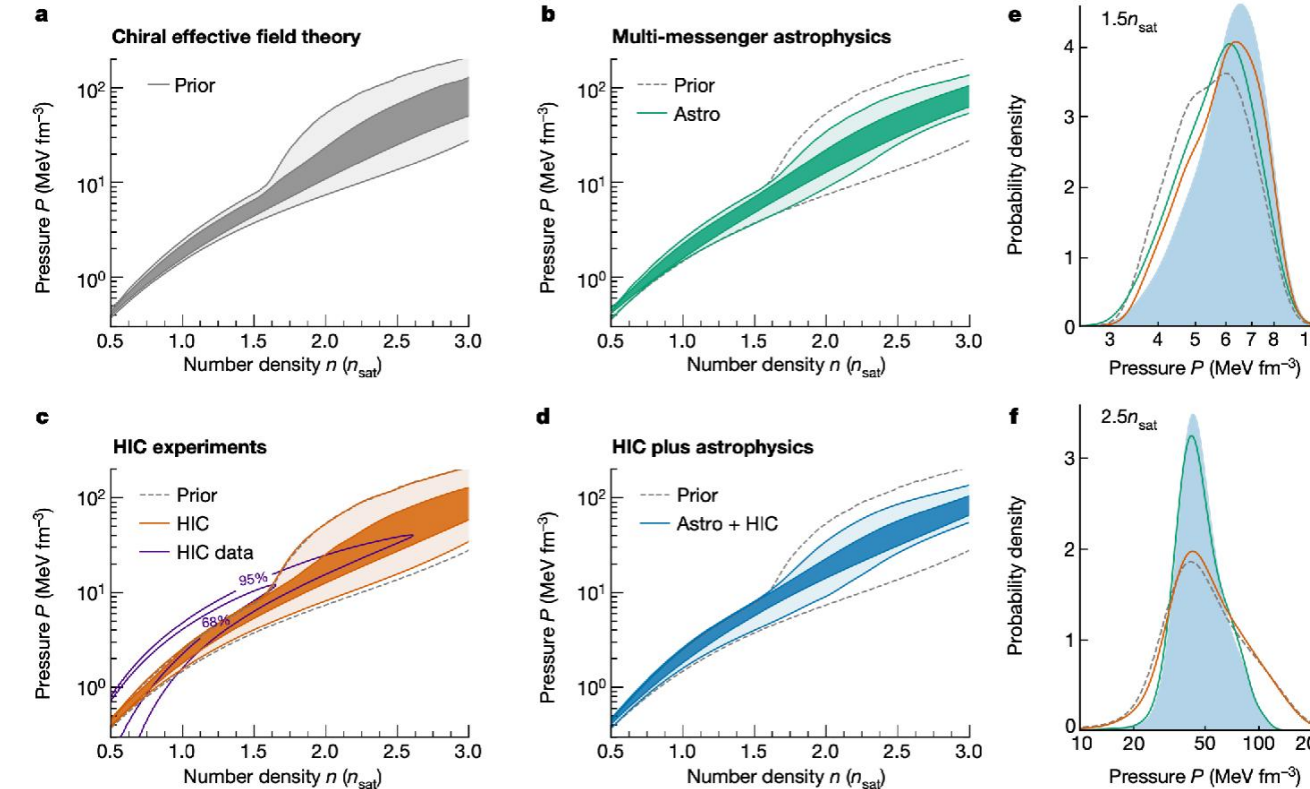
off-diagonal = misclassified



PLB 822 (2021) 136669, Y.J Wang, F.P. Li, Q.F. Li, H.L. Lü, and K. Zhou

Bayesian analysis dense Nuclear EoS

through micro and macro collisions



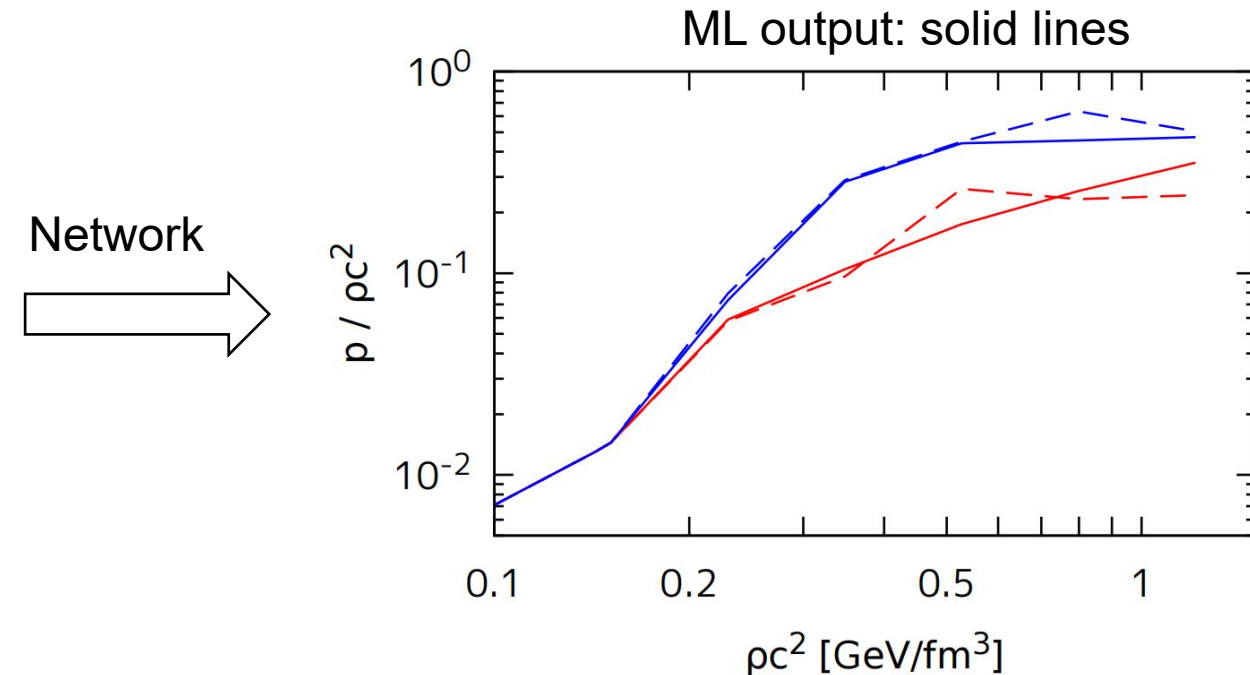
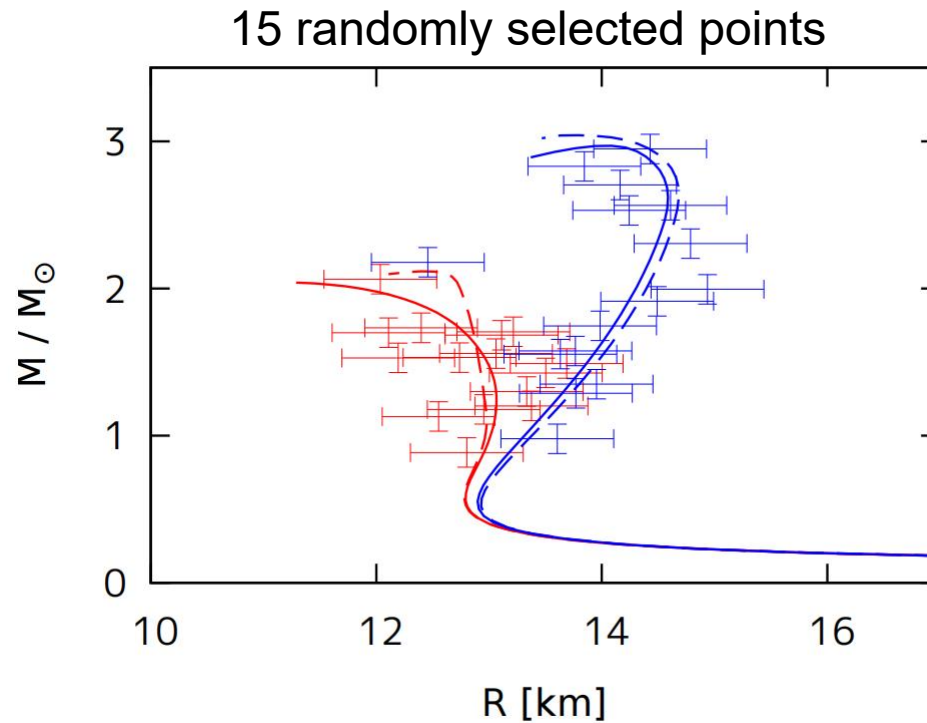
Left: Bayesian Inference Dense Matter EoS from HIC and astrophysics

Right: Bayesian Inference Dense Matter EoS from HIC using model (UrQMD) data comparison

S. Huth et al., Nature 606, 276 (2022)

M.OK, J. Steinheimer, K. Zhou, H. Stoecker, PRL131,202303(2023)

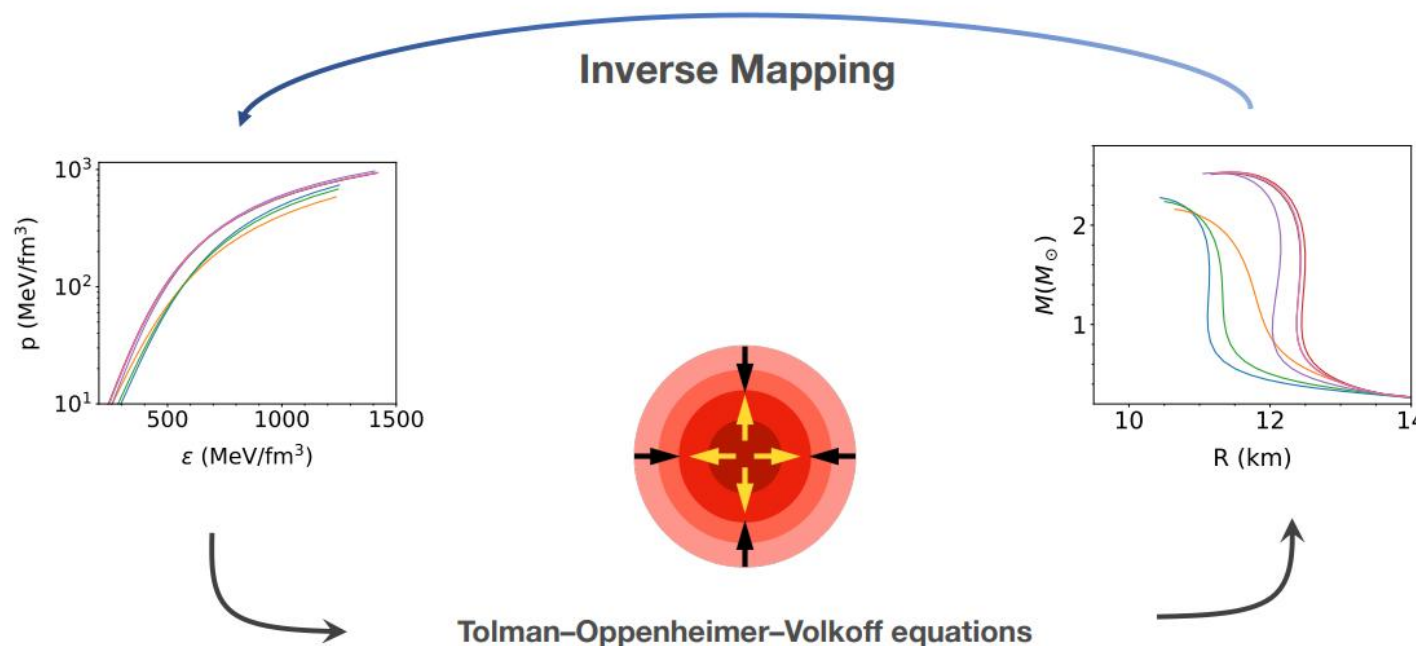
TOV equation and nuclear EoS from DL



Yuki Fujimoto, Kenji Fukushima, and Koichi Murase, PRD 98 (2018) 2, 023019

TOV Equation and Nuclear EoS from DL

$$\frac{dp}{dr} = -G \frac{m(r)\varepsilon(r)}{r^2} \left(1 + \frac{p(r)}{\varepsilon(r)}\right) \left(1 + \frac{4\pi r^3 p(r)}{m(r)}\right) \left(1 - \frac{2Gm(r)}{r}\right)^{-1},$$
$$\frac{dm}{dr} = 4\pi r^2 \varepsilon,$$



S. Soma, L. Wang, S. Shi, H. Stöcker, K. Zhou, PRD 107, (2023) 083028

Auto Differentiation: machine precision

- Forward Mode

Introduce dual numbers: $x \rightarrow x + \dot{x}\mathbf{d}$

where $\mathbf{d}^2 = 0$

$$(x + \dot{x}\mathbf{d}) + (y + \dot{y}\mathbf{d}) = x + y + (\dot{x} + \dot{y})\mathbf{d}$$

$$(x + \dot{x}\mathbf{d}) - (y + \dot{y}\mathbf{d}) = x - y + (\dot{x} - \dot{y})\mathbf{d}$$

$$(x + \dot{x}\mathbf{d}) * (y + \dot{y}\mathbf{d}) = xy + (x\dot{y} + \dot{x}y)\mathbf{d}$$

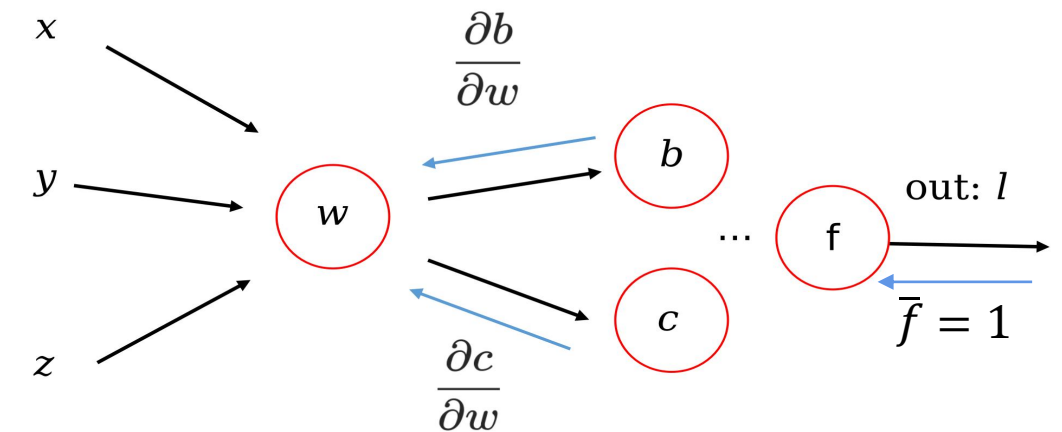
$$\frac{1}{x + \dot{x}\mathbf{d}} = \frac{1}{x} - \frac{\dot{x}}{x^2}\mathbf{d} \quad (x \neq 0)$$

Forward mode for $R^1 \rightarrow R^n$

Reverse mode for $R^n \rightarrow R^1$

- Reverse Mode

adjoint number: $\bar{w} = \frac{\partial l}{\partial w}$

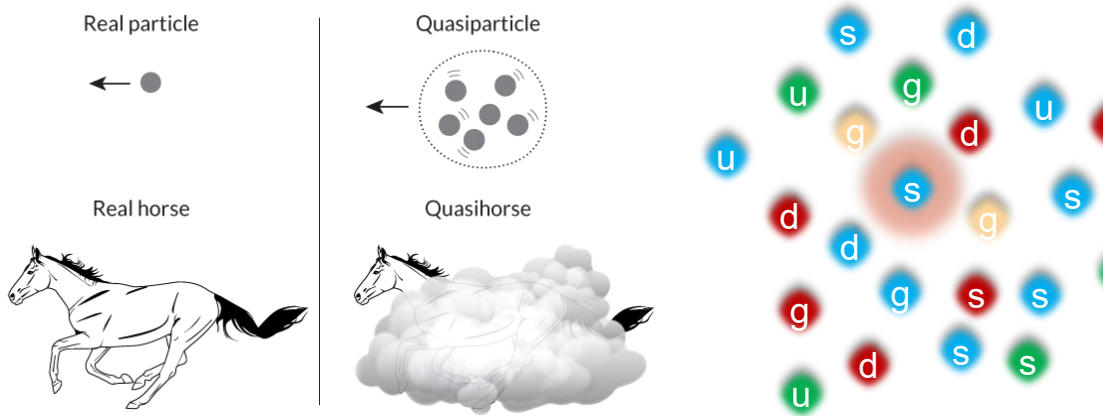


$$\text{step 1 : } \bar{w} = 0$$

$$\text{step 2 : } \bar{w} = \bar{w} + \bar{b} \frac{\partial b}{\partial w}$$

$$\text{step 3 : } \bar{w} = \bar{w} + \bar{c} \frac{\partial c}{\partial w}$$

Deep Learning Quasi Particle Model

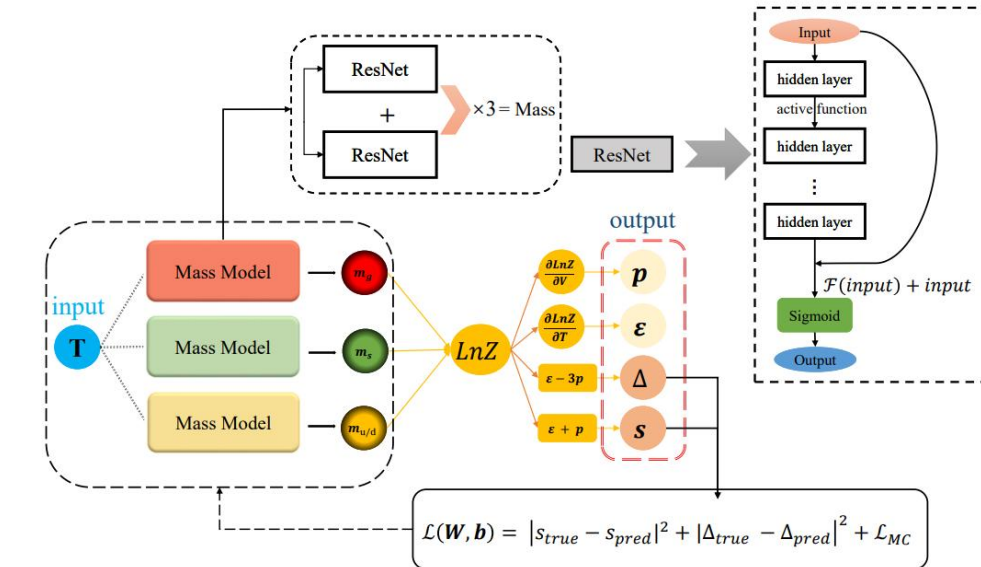


$$\ln Z(T) = \ln Z_g(T) + \ln Z_{u,d}(T) + \ln Z_s(T),$$

Fermi-Dirac distributions,

$$\ln Z_g(T) = -\frac{16V}{2\pi^2} \int_0^\infty p^2 dp \ln \left[1 - \exp \left(-\frac{1}{T} \sqrt{p^2 + m_g^2(T)} \right) \right], \quad (2)$$

$$\ln Z_{q_i}(T) = +\frac{12V}{2\pi^2} \int_0^\infty p^2 dp \ln \left[1 + \exp \left(-\frac{1}{T} \sqrt{p^2 + m_{q_i}^2(T)} \right) \right], \quad (3)$$



quarks, $m_s(T, \theta_2)$ for strange quark and $m_g(T, \theta_3)$ for gluons, where θ_1 , θ_2 and θ_3 are the parameters in DNN shown in Fig. 1.

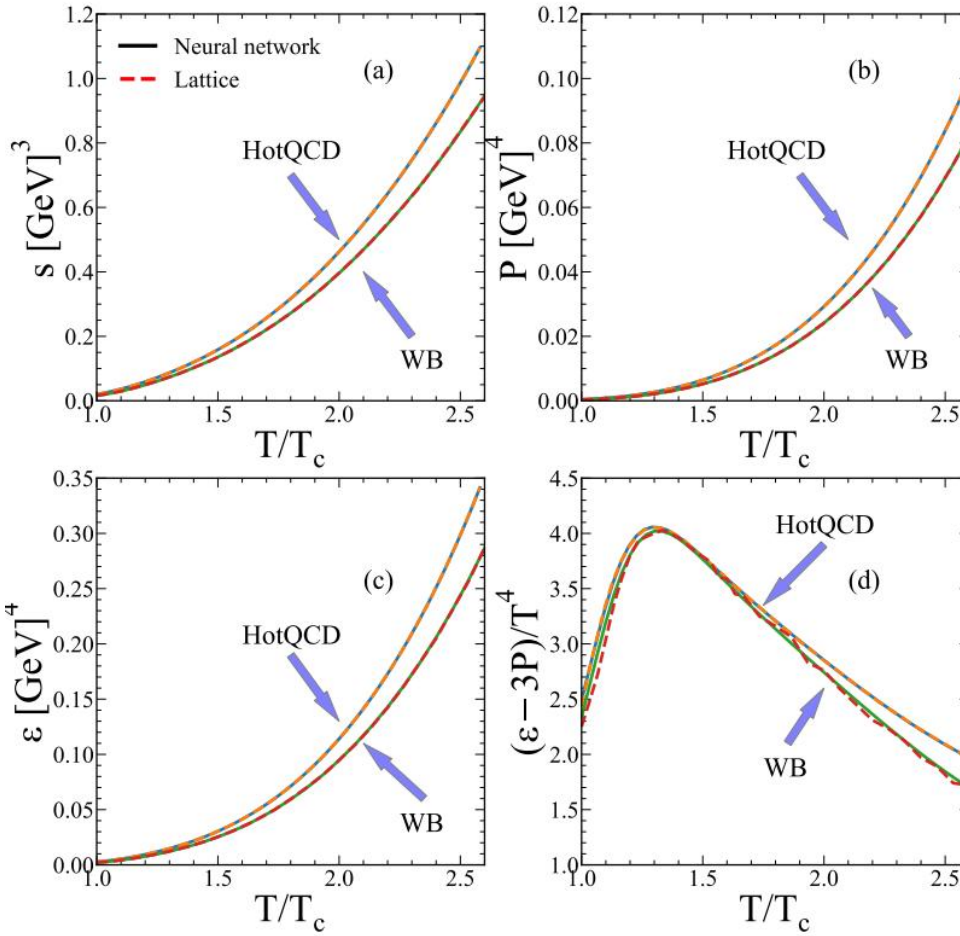
The resulting pressure and energy density are computed using the following statistical formulae,

$$P(T) = T \left(\frac{\partial \ln Z(T)}{\partial V} \right)_T, \quad (5)$$

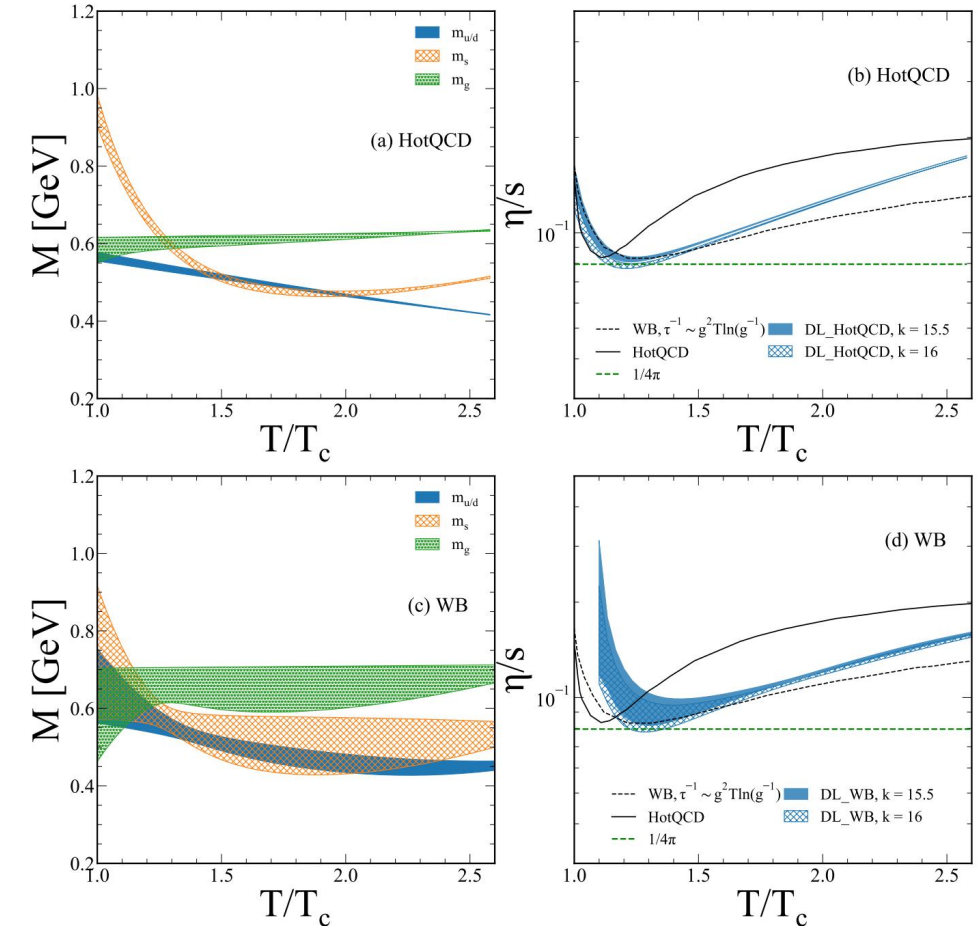
$$\epsilon(T) = \frac{T^2}{V} \left(\frac{\partial \ln Z(T)}{\partial T} \right)_V, \quad (6)$$

The learned quasi parton mass

EoS vs Lattice QCD



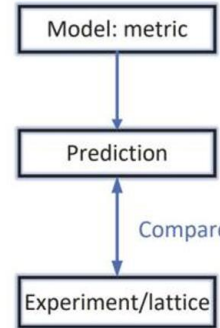
Learned Mass



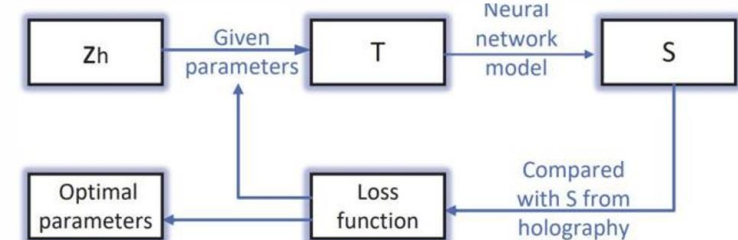
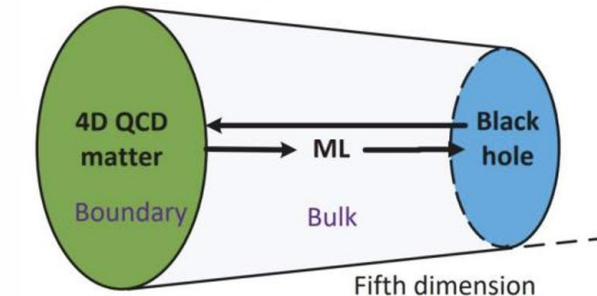
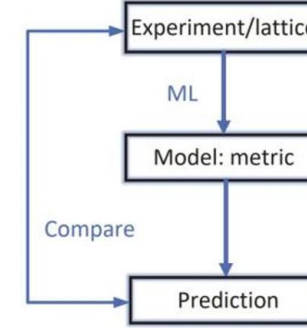
FuPeng Li, HL Lu, LG Pang, GY Qin, PLB 2023; Extend to finite μ_B , arXiv:2501.1001

DL for holographic model using PINN

Conventional Holographic model:



ML Holographic model:



Einstein-Maxwell-Dilation model

O. DeWolfe, S. S. Gubser, and C. Rosen, Phys. Rev. D 83, 086005 (2011), arXiv:1012.1864.

Action:

$$S_B = \frac{1}{16\pi G_5} \int d^5x \left[\sqrt{-g}R - \frac{f(\phi)}{4}F^2 - \frac{1}{2}\partial_\mu\phi\partial^\mu\phi - V(\phi) \right]$$

Non-conformal

ϕ is dilaton

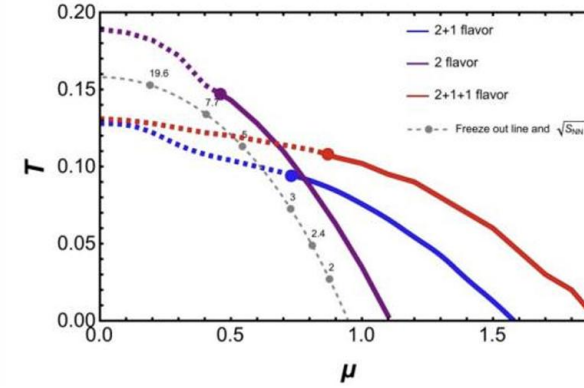
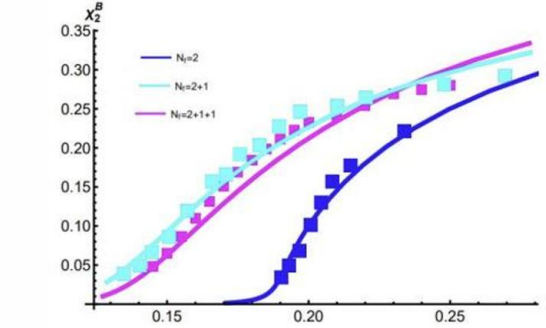
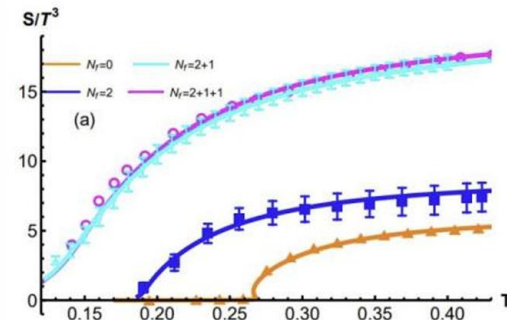
F is the tensor of gauge field

Metric ansatz:

$$ds^2 = \frac{e^{2A(z)}}{z^2} \left[-g(z)dt^2 + \frac{dz^2}{g(z)} + d\vec{x}^2 \right]$$

$$A(z) = d\ln(az^2 + 1) + d\ln(bz^4 + 1), \quad f(z) = e^{cz^2 - A(z) + k}$$

$$s = \frac{e^{3A(z_h)}}{4G_5 z_h^3}, \quad \chi_2^B = \frac{1}{T^2} \frac{\partial \rho}{\partial \mu}.$$



X. Chen, M. Huang, Phys.Rev.D 109 (2024) L051902; JHEP02 (2025) 123

Stacked U-net for relativistic hydro

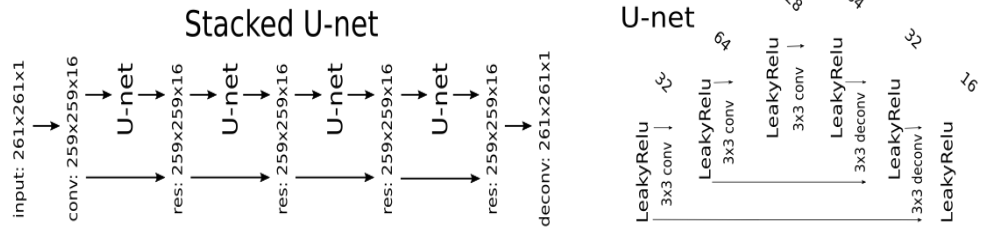
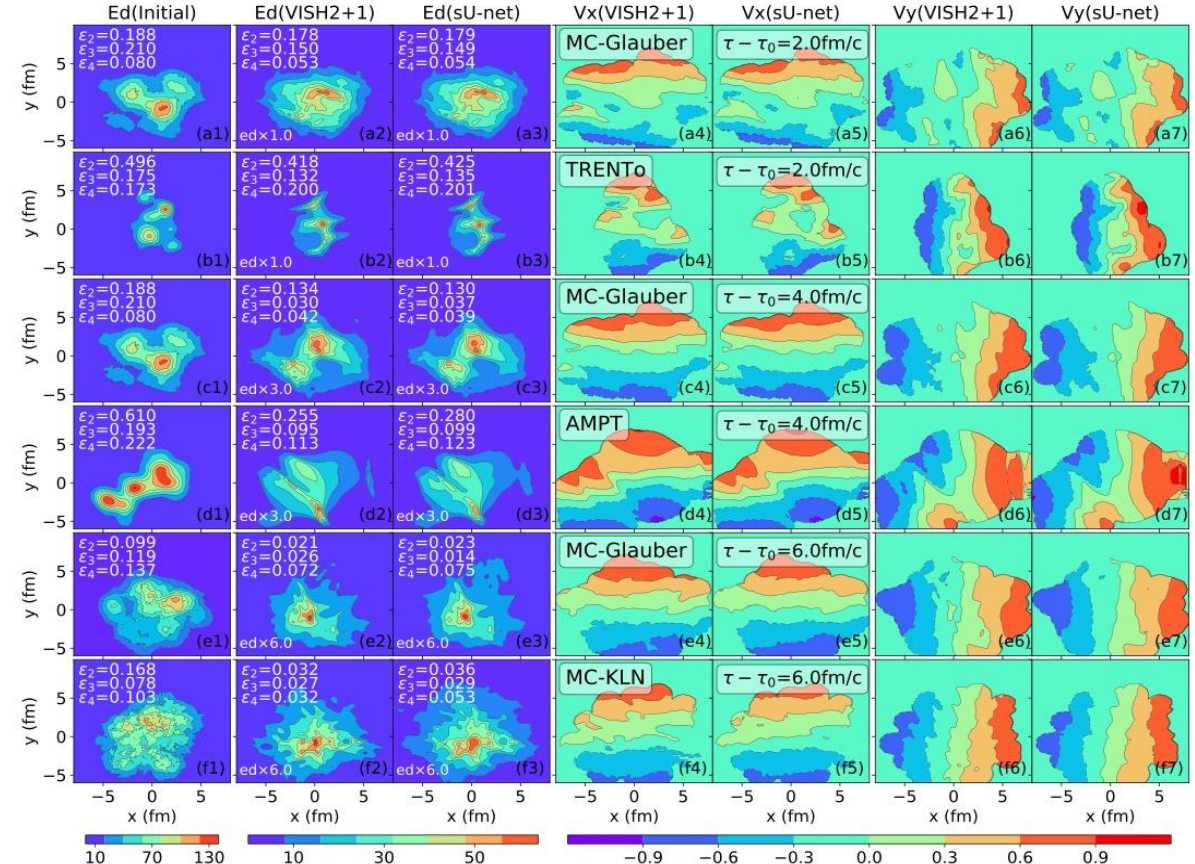
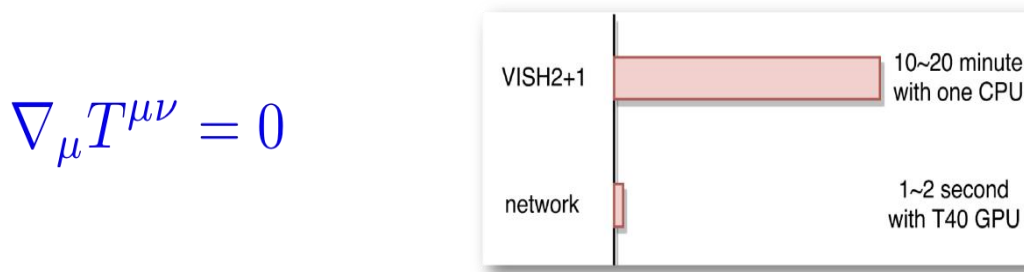


FIG. 1: An illustration of the encode-decode network, **stacked U-net**, which consists of the input and out layers and four residual U-net blocks. The right figure shows the U-net structure, and the depth of the hidden layer is written on the top of them.

The expansion of quark gluon plasma is learned in the image translation task using stacked UNET.



PRR. 3 (2021) 2, 023256, H.Huang, B.Xiao, H.Xiong, Z.Wu, Y. Mu and H.Song

Medium response for nuclear EoS

$$p \partial f(p) = -C(p) \quad (p \cdot u > p_{cut}^0)$$

$$\partial_\mu T^{\mu\nu}(x) = j^\nu(x)$$

$$j^\nu = \sum_i p_i^\nu \delta^{(4)}(x - x_i) \theta(p_{cut}^0 - p \cdot u)$$

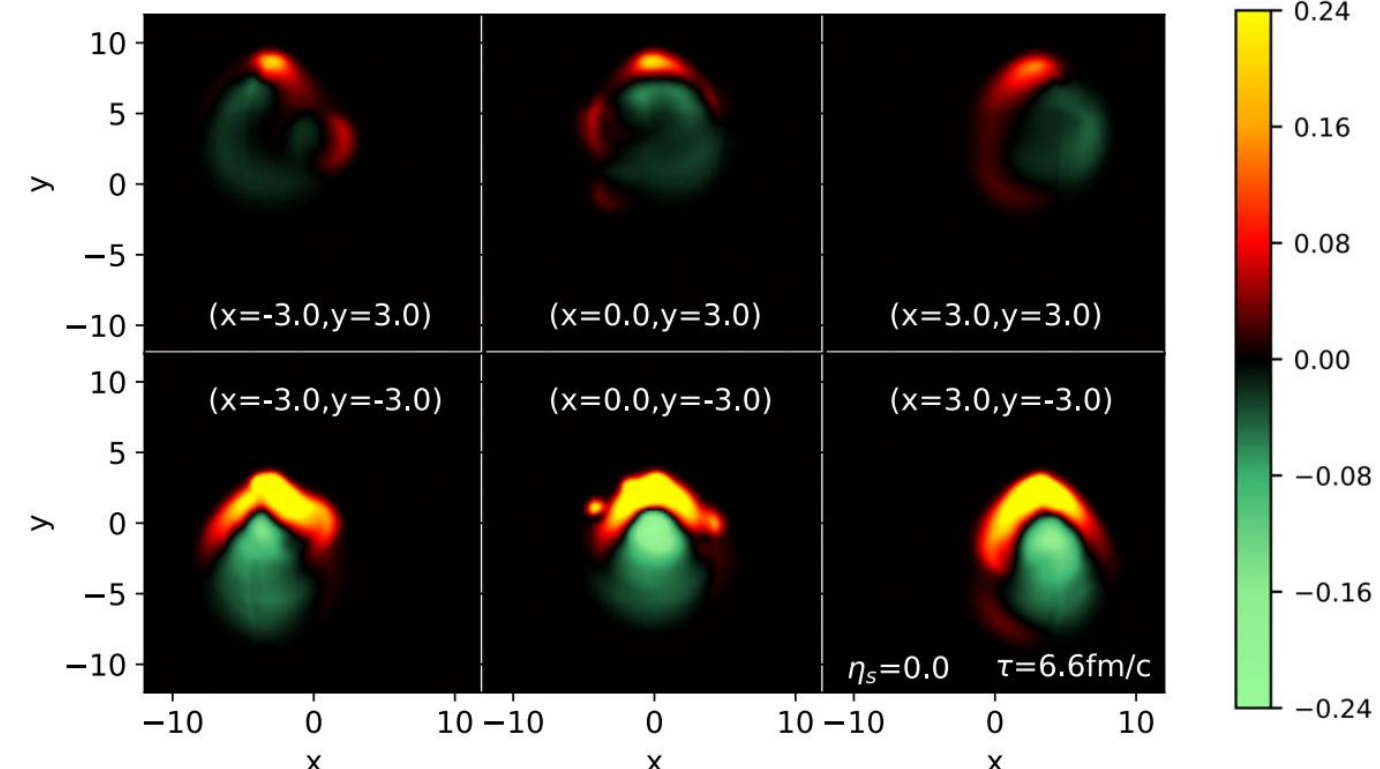
LBT: YY He, T Luo, XN Wang, Y Zhu,
 PRC 91 (2015) 054908, PRC 97 (2018) 1, 019902

CLVisc:

LG Pang, Q Wang, XN Wang, PRC 86 (2012) 024911

LG Pang, H Petersen, XN Wang, PRC 97 (2018) 6,
 064918

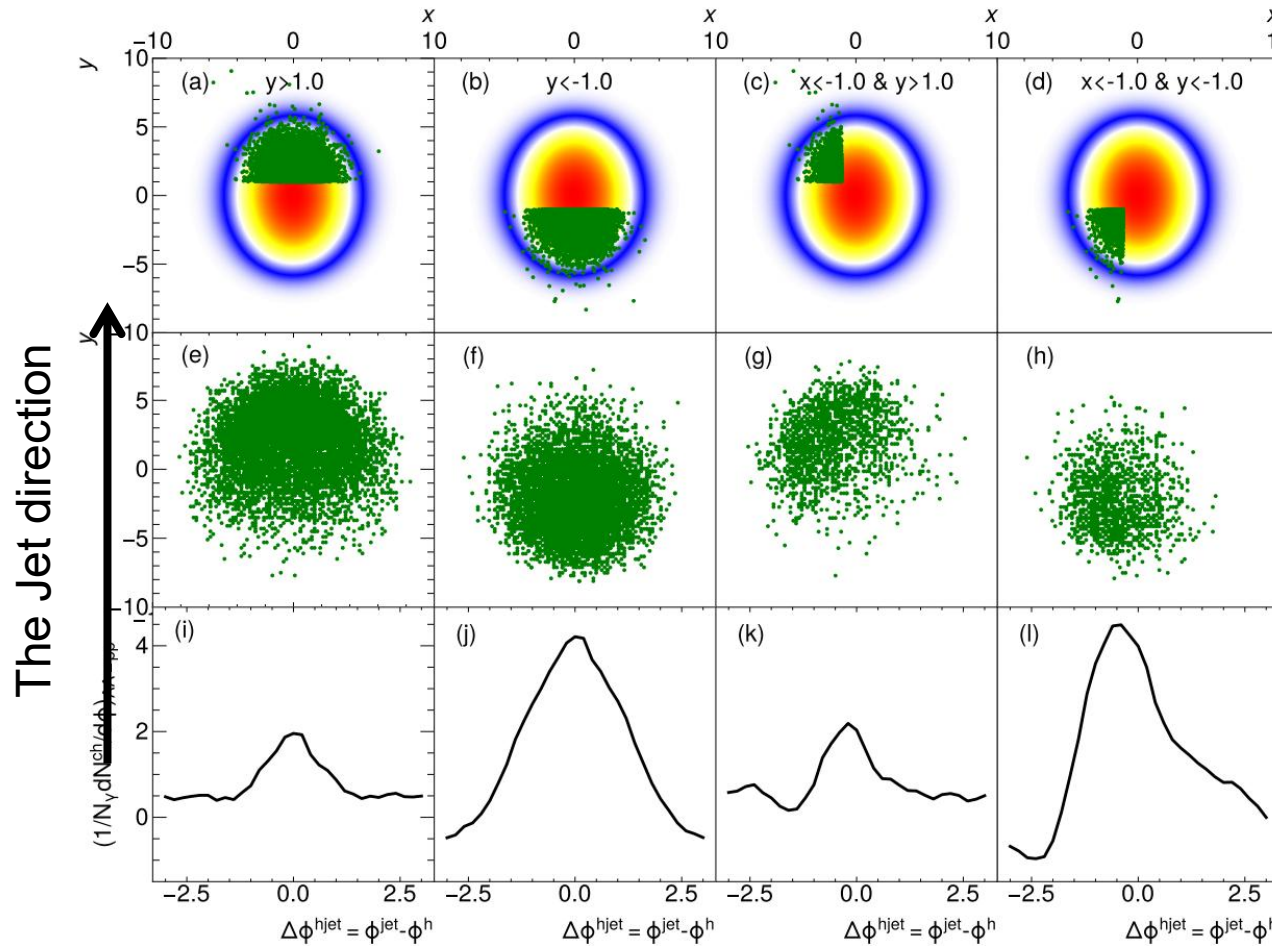
XY Wu, GY Qin, LG Pang, XN Wang, PRC 105 (2022)
 3, 034909



CoLBT:

W Chen, T Luo, SS Cao, LG Pang, XN Wang,
 PLB 777 (2018) 86-90

DL assisted jet tomography



Network predictions

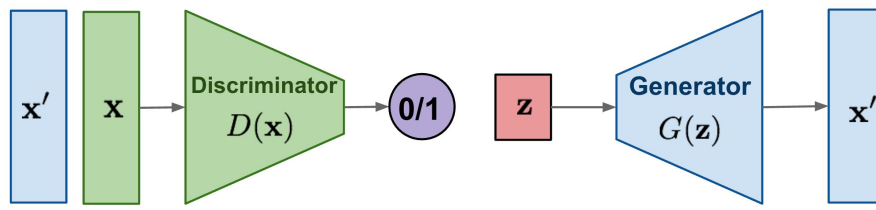
True locations

Jet hadron correlation for selected events whose locations are constrained to specific regions using DL assisted jet tomography

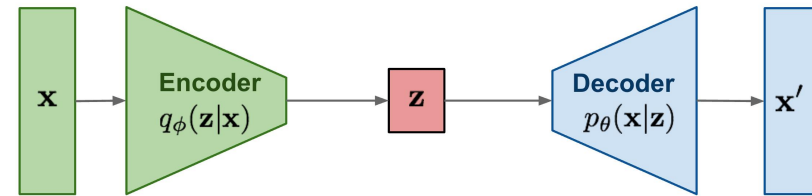
Z Yang, YY He, W Chen, WY Ke, LG Pang, XN Wang, EPJC 83 (2023) 7, 652
Z Yang, T Luo, W Chen, LG Pang, XN Wang, PRL 130 (2023) 5, 052301

Generative models: MC sampling

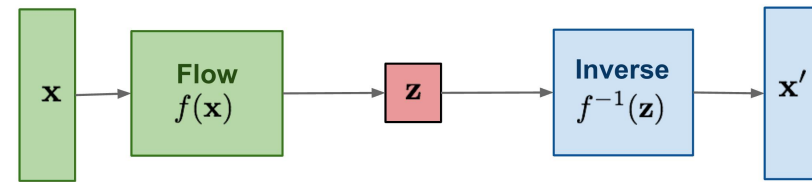
GAN: Adversarial training



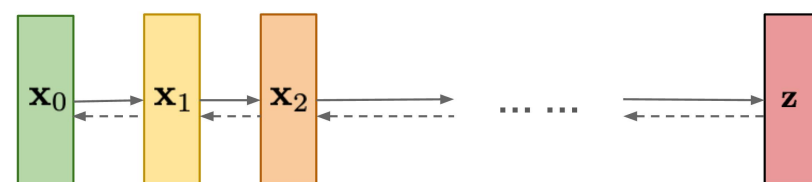
VAE: maximize variational lower bound



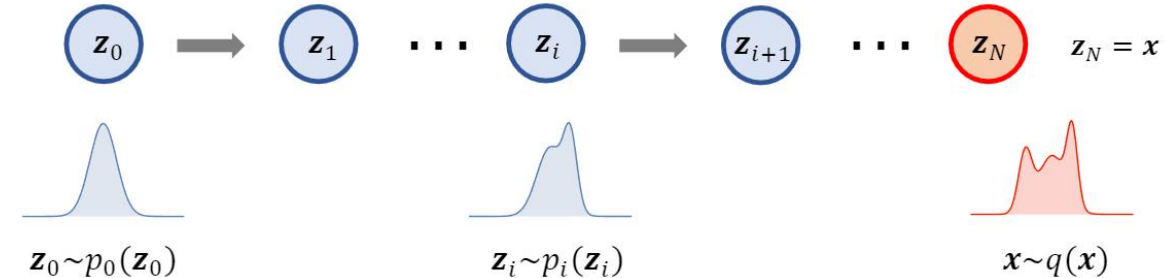
Flow-based models:
Invertible transform of distributions



Diffusion models:
Gradually add Gaussian noise and then reverse

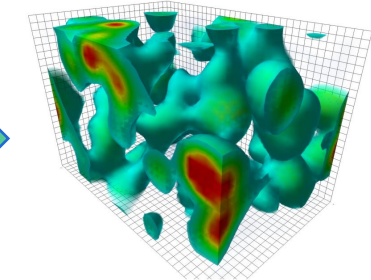


Similar to Box Muller algorithm



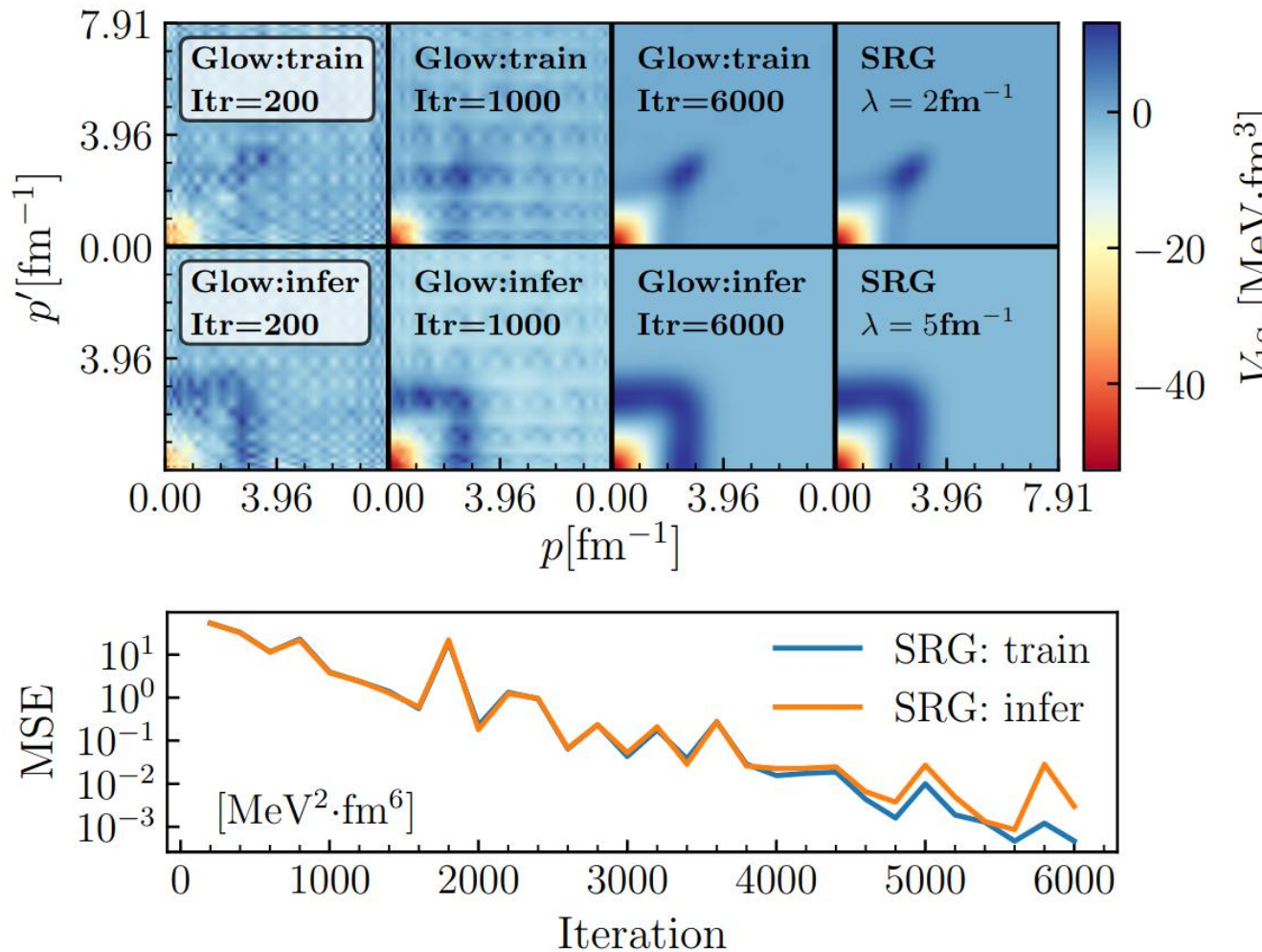
Samples Drawn from N-Dim Normal Distribution

Flow model or Diffusion models



Flow-based generative models for Markov chain Monte Carlo in lattice field theory
Albergo, Kanwar, Shanahan 1904.1207

Learn NN interaction potential



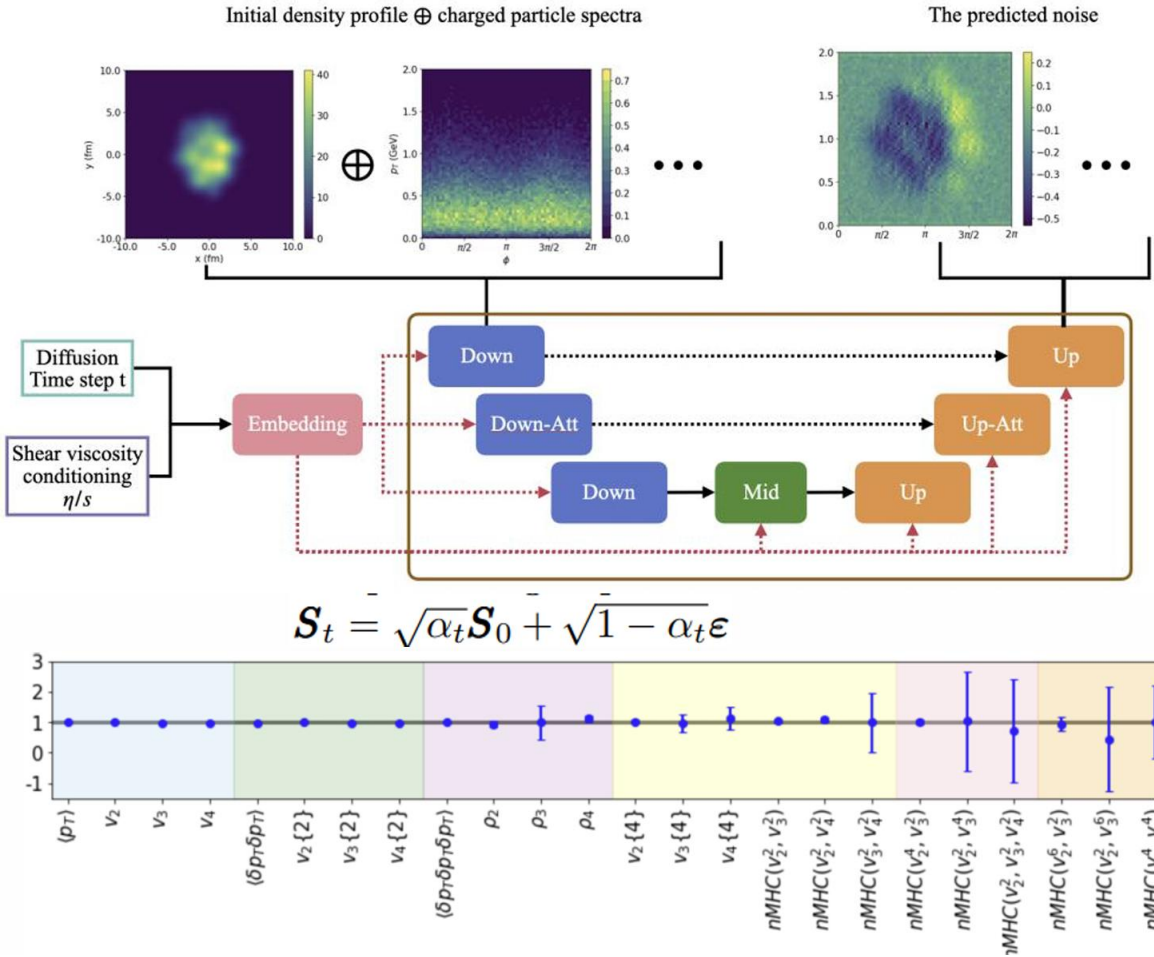
train the **generative model on nucleon-nucleon potentials derived at second and third order in chiral effective field theory** and at three different choices of the resolution scale. We then show that the model can be used to generate samples of the nucleon-nucleon potential drawn from a continuous distribution in the resolution scale parameter space. The generated potentials are shown to produce high-quality nucleon-nucleon scattering phas

Generative model for HICs

An end-to-end generative diffusion model for heavy-ion collisions

[arXiv:2410.13069](https://arxiv.org/abs/2410.13069)

Jing-An Sun,^{1,2} Li Yan,^{1,3} Charles Gale,² and Sangyong Jeon²



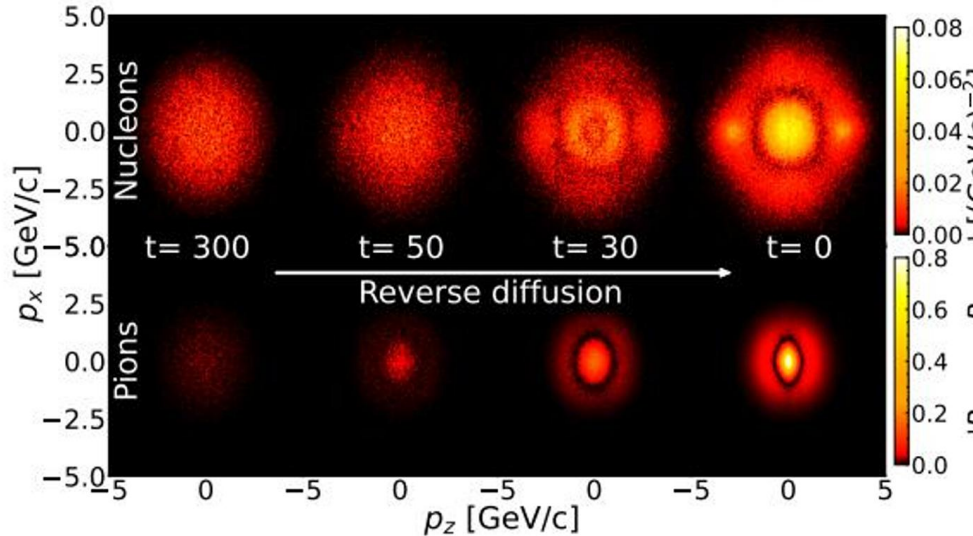
tor. We carried out (2+1)D minimum bias simulations of Pb-Pb collisions at 5.02 TeV, choosing the shear viscosity η/s to be one of three distinct values: 0.0, 0.1, and 0.2. For each value of η/s , we generate 12,000 pairs of initial entropy density profiles and final particle spectra corresponding to 12,000 simulated events, as the training dataset. 70% of the total events are used for training and the rest are used for validation.

Considering that the spectra \mathbf{S}_0 depend on the initial entropy density profiles \mathbf{I} and the shear viscosity η/s , we train a conditional reverse diffusion process $p(\mathbf{S}_0|\mathbf{I}, \eta/s)$ without modifying the forward process.

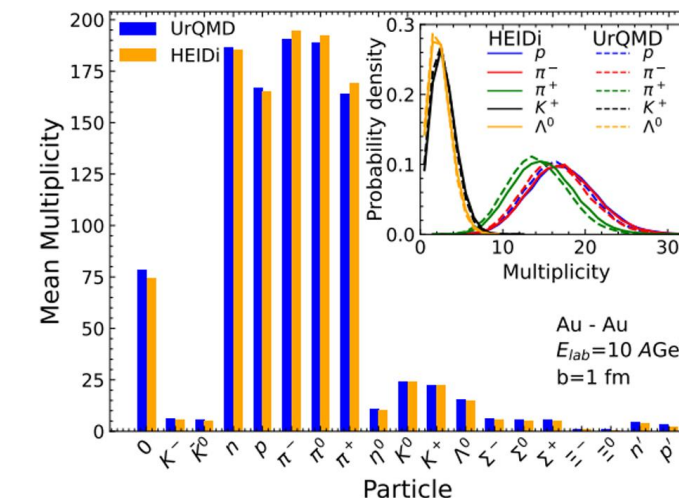
one single central collision event in just 10^{-1} seconds on a GeForce GTX 4090 GPU.

ble precision, as the traditional numerical simulation of hydrodynamics for one central event typically takes approximately 120 minutes (10^4 seconds) on a single CPU.

Generative model for HICs



M. O.K, K. Z, J. S, H. S, arXiv: 2502.16330, arXiv:2412.10352

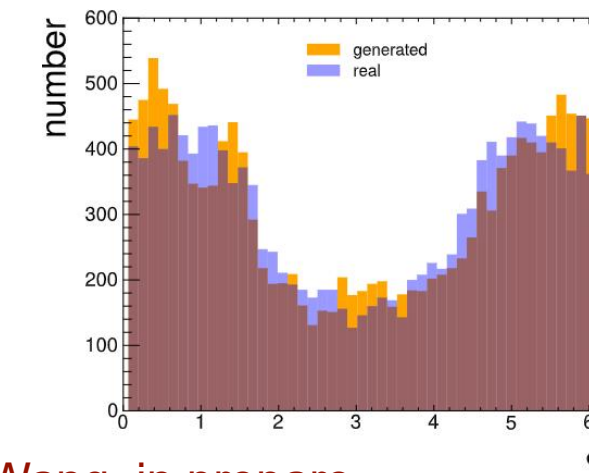
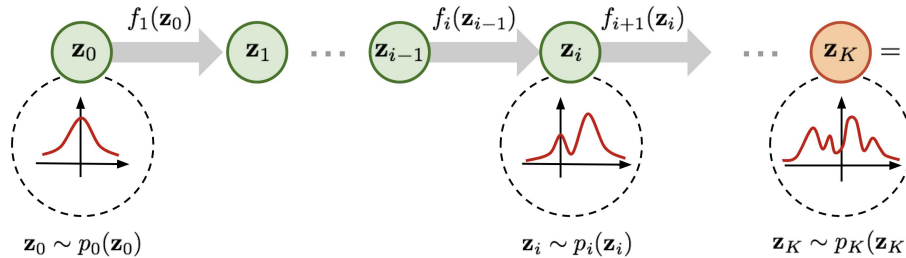


18k **UrQMD** simulation events for training

HEIDI:
Heavy-ion Events through Intelligent Diffusion

PointNet encoder +
Normalizing flow decoder +
Pointcloud diffusion

credit: <https://lilianweng.github.io/>



Event-by-event jet loss and medium response

Flow model and flow matching are used to learn the high dimensional distribution for faster medium response sampler

K.Y. Wu, Z. Yang, L.G. Pang and X.N. Wang, in prepare



Review articles

nature reviews physics

<https://doi.org/10.1038/s42254-024-00798-x>

Nature Review Physics (2025)

Perspective

Check for updates

Physics-driven learning for inverse problems in quantum chromodynamics

Gert Aarts¹, Kenji Fukushima², Tetsuo Hatsuda³, Andreas Ipp⁴, Shuzhe Shi⁵, Lingxiao Wang³✉ & Kai Zhou^{6,7}

Abstract

The integration of deep learning techniques and physics-driven designs is reforming the way we address inverse problems, in which accurate physical properties are extracted from complex observations. This is particularly relevant for quantum chromodynamics (QCD) – the theory of strong interactions – with its inherent challenges in interpreting

Sections

- Introduction
- Physics-driven learning
- QCD physics
- Conclusions and outlook

Review Of Modern Physics (2022)

Colloquium: Machine learning in nuclear physics

Amber Boehlein, Markus Diefenthaler, Nobuo Sato, Malachi Schram, Veronique Ziegler, Cristiano Morten Hjorth-Jensen, Tanja Horn, Michelle P. Kuchera, Dean Lee, Witold Nazarewicz, Peter Ostroff, Orginos, Alan Poon, Xin-Nian Wang, Alexander Scheinker, Michael S. Smith, and Long-Gang Pang
Rev. Mod. Phys. **94**, 031003 – Published 8 September 2022

Article

References

No Citing Articles

PDF

HTML

Export Citation

Prog. Part. Nucl. Phys. 135 (2024) 104084

Contents lists available at [ScienceDirect](#)



ELSEVIER

Progress in Particle and Nuclear Physics

journal homepage: www.elsevier.com/locate/ppnp



Check for updates

Review

Exploring QCD matter in extreme conditions with Machine Learning

Kai Zhou^{a,b,*}, Lingxiao Wang^{a,*}, Long-Gang Pang^{c,*}, Shuzhe Shi^{d,e,*}

^a Frankfurt Institute for Advanced Studies (FIAS), D-60438 Frankfurt am Main, Germany

^b School of Science and Engineering, The Chinese University of Hong Kong, Shenzhen 518172, China

^c Institute of Particle Physics and Key Laboratory of Quark and Lepton Physics (MOE), Central China Normal University, Wuhan, 430084, China

^d Department of Physics, Tsinghua University, Beijing 100084, China

Nuclear Science and Techniques (2023) 34:88

<https://doi.org/10.1007/s41365-023-01233-z>

REVIEW ARTICLE

Nucl. Sci. Tech. 34 (2023) 6, 88

High-energy nuclear physics meets machine learning

Wan-Bing He^{1,2}✉ · Yu-Gang Ma^{1,2}✉ · Long-Gang Pang³✉ · Hui-Chao Song⁴✉ · Kai Zhou⁵✉

: 18 April 2023 / Published online: 21 June 2023

Thank you!

Science China Physics, Mechanics & Astronomy
Machine learning in nuclear physics at low and intermediate energies

Wanbing He,^{1, 2, *} Qingfeng Li,^{3, 4, †} Yugang Ma,^{1, 2, ‡} Zhongming Niu,^{5, §} Junchen Pei,^{6, 7, ¶} and Yingxun Zhang^{8, 9, **}